

**REPUBLIC OF TURKEY
AYDIN ADNAN MENDERES UNIVERSITY
GRADUATE SCHOOL OF NATURAL AND APPLIED SCIENCES
MECHANICAL ENGINEERING
2020-M.Sc.-006**



**MATERIAL OPTIMIZATION FOR
LADDER CLIMBING ROBOT**

Ogulcan TURHANLAR

Supervisor:

Prof. Dr. Ismail BOGREKCI

AYDIN

REPUBLIC OF TURKEY
AYDIN ADNAN MENDERES UNIVERSITY
GRADUATE SCHOOL OF NATURAL AND APPLIED SCIENCES
AYDIN

The thesis with the title of “Material Optimization for Ladder Climbing Robot” prepared by the Ogulcan TURHANLAR, Master Student at the Mechanical Engineering Program at the Department of Mechanical Engineering was accepted by the jury members whose names and titles presented below as a result of thesis defense on 13.01.2020.

	Title, Name Surname	Institution	Signature
President :	Prof. Dr. Ismail BOGREKCI	Aydin Adnan Menderes University	
Member :	Prof. Dr. Zeki KIRAL	Dokuz Eylul University	
Member :	Prof. Dr. Hasan OZTURK	Dokuz Eylul University	

This Master Thesis accepted by the jury members is endorsed by the decision of the Institute Board Members with Serial Number and date.

Prof. Dr. Gönül AYDIN
Institute Director

REPUBLIC OF TURKEY
AYDIN ADNAN MENDERES UNIVERSITY
GRADUATE SCHOOL OF NATURAL AND APPLIED SCIENCES
AYDIN

I hereby declare that all information and results reported in this thesis have been obtained by my part as a result of truthful experiments and observations carried out by the scientific methods, and that I referenced appropriately and completely all data, thought, result information which do not belong my part within this study by virtue of scientific ethical codes.

13 /01/2020

Ogulcan TURHANLAR

ÖZET

MERDİVEN TIRMANAN ROBOT İÇİN MALZEME OPTİMİZASYONU

Oğulcan TURHANLAR

Yüksek Lisans Tezi, Makine Mühendisliği Anabilim Dalı

Tez Danışmanı: Prof. Dr. İsmail BÖĞREKÇİ

2020, 92 sayfa

Bu tez çalışmasında, merdiven çıkma, engele tırmanabilme yeteneklerine sahip bir robotik sistem tasarlanmış, gerekli analitik hesaplamalar ve nümerik analizler uygulanmıştır. Tasarlanan robotik sistem evsel ve endüstriyel çalışma alanlarına uygundur. Bu amaçla, robotun hareket sistemi hibrit olacak şekilde planlanmıştır. Hibrit hareket sistemi üç tekerlek ve bu üç tekerleğin birleşimi ile hareket edebilen bacaklar ile oluşturulmuştur. Analitik hesaplamalar kısmında, belirlenen yapı elemanları (kaplin, şaftlar) S235, diğer yapı elemanları PLA malzeme ile modellenmiş ve hesaplamalar doğrultusunda sistemin güç, tork ve ivme değerleri bulunmuştur. Aynı malzeme konfigürasyonu nümerik analiz yazılımı ANSYS Rigid Body Dynamics modülünde modellenerek sonlu elemanlar yöntemi ile hesaplanmış ve benzer sonuçlar elde edilmiştir. Bu kıyaslama işlemi ile modellemenin doğrulanmasının ardından tork, güç ve ivme değerleri nümerik hesaplamalar ile S235, Al6061, PLA ve ABS malzemelerinden oluşan şase için uygulanmıştır. Elde edilen değerler sistemin kritik bileşenleri olarak belirlenen iç şaft, merkez şaft ve dış dişli parçalarına uygulanarak malzeme dayanımları incelenmiştir. Bu çalışmalar doğrultusunda tasarımı gerçekleştirilen merdiven tırmanan robot şasesinin, mekanik dayanımlar ve enerji verimliliği göz önünde bulundurularak PLA malzemesinden üretilmesi uygun bulunmuştur. Geliştirilen sistemin çalışmasında 67.5 Watt güç ihtiyacı olacağı hesaplanmıştır.

Anahtar Kelimeler: Analitik Hesaplamalar, Dayanım ve Verimlilik Tabanlı Tasarım Optimizasyonu, Malzeme Seçimi, Merdiven Tırmanan Robot, Nümerik Hesaplamalar.

ABSTRACT

MATERIAL OPTIMIZATION FOR LADDER CLIMBING ROBOT

Ogulcan TURHANLAR

M.Sc. Thesis, Department of Mechanical Engineering

Supervisor: Prof. Dr. Ismail BOGREKCI

2020, 92 pages

In this thesis, a robotic system that is capable of obstacle and ladder climbing was designed with utilization of analytical calculations and numerical analysis. Designed robotic system is suitable to work in both domestic and industrial environment. With this purpose, hybrid transitional locomotion mechanism that consists of three wheels and legs was developed. In analytical calculations, robotic system that some structural elements' (coupling, shafts) materials were defined as S235 and other structural elements materials as PLA was modelled to calculate power, acceleration and torque requirement. Same material configuration were modelled to obtain similar outputs and applied to numerical analysis software ANSYS Rigid Body Dynamics. That comparison process between analytical and numerical solutions was used as verification of models. Numerical analysis was applied for chassis of the robot with S235, Al6061, PLA and ABS materials. Obtained results were used to analyze critical components of robot such as inner shaft, main shaft and outer gear to investigate of strength of materials. According to the obtained results from computations & analyses and energy efficiency, it was observed that it was the most suitable and optimum to manufacture the chassis of the robotic system using PLA material. It was also found that the developed system was required 67.5 Watt power in the operation.

Key Words: Analytical Calculations, Design Optimization Basis on Strength and Efficiency, Ladder Climbing Robot, Material Selection, Numerical Analysis.

ACKNOWLEDGEMENTS

I wish to express my gratitude to my supervisor, Prof. Dr. Ismail BOGREKCI who was abundantly helpful and offered invaluable support with his sincerity and belief in me. In addition, I am especially grateful to Prof. Dr. Pinar DEMIRCIOGLU for her useful advices and comments.

I wish to acknowledge for the supports of Hilmi Saygin SUCUOGLU, Neslihan DEMIR, Burak KAYA and Emrah GUVEN.

Additionally, I would like to thank General Director Levent OZYAR and Technical Director Cuneyt ALBAK of MEKTA Company for their valuable supports.

In addition, I would like to thank my lovely family of TURHANLAR for their invaluable efforts when I felt hopeless and weak in solving problems.

Finally, I would like to send my special thanks to my fiancée Ecem EROGLU for her understanding, help and encouragement and faith in me.

Ogulcan TURHANLAR

TABLE OF CONTENTS

ÖZET.....	vii
ABSTRACT.....	ix
ACKNOWLEDGEMENTS.....	xi
TABLE OF CONTENTS.....	xiii
LIST OF FIGURES.....	xv
LIST OF TABLES.....	xix
1. INTRODUCTION.....	1
1.1. Problem Description.....	1
1.2. Motivation.....	1
1.3. Objectives.....	1
1.4. Overview of the Thesis.....	2
2. LITERATURE REVIEW.....	3
2.1. Robot Manipulators.....	4
2.2. Mobile Robots.....	7
2.3. Humanoid Robots.....	16
2.4. Material Selection.....	28
2.4.1. Material Selection Process.....	28
2.4.2. Material of Robot Frame.....	28
3. MATERIAL AND METHOD.....	31
3.1. Design of Drive-Train for Transitional Locomotion Mechanism.....	32

3.2. Design of Robot Structure	36
3.2.1. Design of Linear Actuation Mechanism.....	38
3.3. Verification of Designed System.....	41
3.3.1. Analytical Calculations for Ladder Climbing Robot.....	42
3.3.2. Numerical Analysis for Ladder Climbing Robot.....	57
4. RESULTS AND DISCUSSION.....	61
4.1. Verification of Motion Modelling and Analytical Calculation	61
4.2. Numerical Analyses for Motion Calculations	62
4.3. Numerical Analyses for Mechanical Strength.....	63
5. CONCLUSIONS	67
6. RECOMMENDATIONS AND FUTURE WORKS	69
REFERENCES	70
APPENDICES	74
Appendix 1 (Matlab Scripts)	74
Motion Calculations	74
Mechanical Strength Check of the Components	80
RESUME.....	91

LIST OF FIGURES

Figure 2.1 The Robot Boat (A) Patent Drawing (B) Structure (Rosheim, 1994).....	4
Figure 2.2 Unimate Robot (Karl, 2010)	6
Figure 2.3 Operational Stocks of Industrial Robots (IFR World Robotics, 2018)...	6
Figure 2.4 Annual Supply of Industrial Robots According To Usage Fields (IFR World Robotics, 2018).....	7
Figure 2.5 Annual Supply of Industrial Robots According To Continents (IFR World Robotics, 2018).....	7
Figure 2.6 Mobile Robot Samples (A) Aerial Rescue Robot (B) Underwater Robot (C) Mobile Delivery Robot (Chen et al., 2009).	8
Figure 2.7 Model of Mobile Robot's Functional Parts (Chen et al., 2009).....	8
Figure 2.8 Grey Walter's Turtle (Arkin, 1998).	12
Figure 2.9 Shakey Robot (Arkin, 1998).....	12
Figure 2.10 Stanford Cart (Nehmzow, 2003).....	12
Figure 2.11 Genghis Khan Robot (Brooks and Flynn, 1989).	13
Figure 2.12 Khepera Robot (Lund and Miglino, 1996).	13
Figure 2.13 Stanley (Thrun et al., 2006).	13
Figure 2.14 Sojourner or Rover (Mars Rover, 2019).....	13
Figure 2.15 SandFlea (Boston Dynamics, 2019).	14
Figure 2.16 Pioneer (Nasa, 2019).....	14
Figure 2.17 Mobile Robots Used In Agriculture: a) Bonirob Developed By BOSCH Deepfield-Robotics (Bosh, 2019), b) Thorvald was Designed By SAGA ROBOTICS (Saga Robotics, 2019).	15

Figure 2.18 Husky with Mechanisms That Make Him Prepared To Detect Mines (Cabrita Et Al., 2015).....	15
Figure 2.19 Mobile Service Robots Sales for Professional Usage And Forecast Between 2016-2021 (IFR World Robotics, 2018).....	16
Figure 2.20 Mobile Service Robots Sales for Domestic Usage (IFR World Robotics, 2018).....	16
Figure 2.21 The First Dynamically Settled System (Santos et al., 2006).....	17
Figure 2.22 Gait Types (A) Statically Stettled Gait (B) Dynamically Settled Gait (Garcia et al., 2007).....	18
Figure 2.23 Knight In the Armor and Its Inner Mechanism (Silva and Machado, 2007).....	19
Figure 2.24 Mechanical Horse (Nonami et al., 2014)	19
Figure 2.25 Steam Man (Silva and Machado, 2007).....	19
Figure 2.26 General Electric Quadruped (Kar, 2003)	20
Figure 2.27 Phony Pony (Reeve and Hallamr, 2005).....	20
Figure 2.28 The Big Muskie (Silva and Machado, 2007)	21
Figure 2.29 OSU Hexapod (Ozguner and Tsai, 1985)	21
Figure 2.30 Tokyo Institute of Technology Robot Series (a) PV-II (b) TITAN-III (c) TITAN-XI (Nonami et al., 2014).....	22
Figure 2.31 Waseda Robot Series (a) WABOT-1 (b) WABOT-2 (Lim and Takanishi, 2006).....	23
Figure 2.32 Honda Robot Series (a) P2 (b) P3 (c) Asimo (Behnke, 2008; Duran and Thill, 2012).....	23
Figure 2.33 Two Passive Mobile Models of Mcgeer (Narukawa et al., 2010).....	24

Figure 2.34 McGeer's Straight Passive Dynamic Walker (Hobbelen and Wisse, 2007)	25
Figure 2.35 CB ² Robot (Minato et al., 2007)	26
Figure 2.36 Geminoid Robot (Nishio et al., 2007).....	26
Figure 2.37 Humanoid Robots (a) Kismet (b) Hubo (c) Repliee Q2 (Park et al., 2005)	27
Figure 2.38 Time evolution of The Robotics Studies (Garcia et al., 2007)	28
Figure 3.1 The Developed Robotic System.....	31
Figure 3.2 Ladder/Obstacle Dimensions in mm.....	32
Figure 3.3 Off-Road Type Wheels (Pololu).....	33
Figure 3.4 Initial Position of Ladder Climbing Mechanism.....	33
Figure 3.5 Climbing Position	34
Figure 3.6 Transmission System of Robotic System with Parameters.....	34
Figure 3.7 Technical Drawing of the Gears	36
Figure 3.8 General System Design.....	37
Figure 3.9 Dimensions of Ladder Climbing Robot in mm.....	38
Figure 3.10 Designed Linear Actuation Mechanism.....	38
Figure 3.11 Designed Motion System.....	39
Figure 3.12 Designed Transmission System	41
Figure 3.13 Rolling Down on an Inclined Plane Assumption.....	43
Figure 3.14 Torque and Acceleration Calculations for Rolling Motion	47
Figure 3.15 Angular Velocity and Power Calculations for Rolling Motion	48

Figure 3.16 Effected Forces of Body 48

Figure 3.17 Angular Velocity, Torque and Power Calculations for Linear Motion 49

Figure 3.18 Occurred Forces on the Gears 50

Figure 3.19 Technical Drawing of the Main Shaft with Shear-and-Moment Diagram 51

Figure 3.20 The Minimum Shaft Diameter Calculation of Main Shaft..... 52

Figure 3.21 Coupling Pin Diameter Calculation 56

Figure 3.22 Motion and Strength Calculator 56

Figure 3.23 Modeling of Ladder Climbing Motion..... 57

Figure 3.24 Output Parameters of Ladder Climbing Motion Analysis 58

Figure 3.25 Modeling of Straight Road Motion 58

Figure 3.26 Constraint Equation for Gear Transmission..... 59

Figure 3.27 Output Parameters of Straight Road Motion Analysis 59

Figure 3.28 Boundary Conditions of Outer Gear 60

Figure 3.29 Boundary Conditions of Main Shaft 60

Figure 4.1 Acceleration Results of System in Numerical Analysis..... 62

Figure 4.2 Results of the Structural Analysis of Inner Shaft..... 64

Figure 4.3 Results of the Structural Analysis of Main Shaft..... 65

Figure 4.4 Results of the Structural Analysis of Gear 66

LIST OF TABLES

Table 2.1 Comparison of Robotic System and People by the means of Properties .9	
Table 3.1 The Dimensions of the Gears35	
Table 3.2 Explanation of Linear Actuation Mechanism Components39	
Table 3.3 Components of Transmission System with Explanation.....40	
Table 3.4 Mechanical Properties of Materials.....42	
Table 4.1 Weight of System for Different Material Configuration.....61	
Table 4.2 Power Requirement and Torque Values For Each Configuration.....63	
Table 4.3 Safety Factor and Occurred Stresses on Inner Shaft64	
Table 4.4 Safety Factor and Occurred Stresses on Main Shaft65	
Table 4.5 Stress and Safety Factor for Inner Gear66	

1. INTRODUCTION

1.1. Problem Description

In mobile robot systems, it is important to reach upper floor in multistory buildings to complete their tasks in full. Although there are several types of robots that is purposed to climb over ladder to reach upper floors, these systems are based on legged actuation systems that causes low speed in straight roads or strike based robots that causes easy to failure mechanism. This type of ladder climbing robots leads us to design a system and select optimum materials for ladder climbing mechanism.

1.2. Motivation

When the relations between this thesis study and real life applications are observed the requirements are listed below;

1. Using a ladder climbing mechanism for mobile robots system will eliminate restrictions of mobile robots in multistory buildings.
2. Mobile robots that is designed using one locomotion systems make concessions from speed or movement ability.
3. Mobile system can be adaptable for many different place; it can be indoor or outdoor according to adjustments and settings.

The listed are motivated to design ladder-climbing robot.

1.3. Objectives

1. To design a mobile robot system for ladder and obstacle climbing.
2. To develop an adaptive three wheel-legged hybrid locomotion mechanism with transitional system for both ladder climbing and straight roads.
3. To consider ladder climbing motion to specify optimum material between S 235, Al 6061, ABS and PLA according to energy efficiency and strength of material.

1.4. Overview of the Thesis

The outline of the thesis is as follows;

In the next chapter "*Literature Review*",

1. Robot manipulators,
2. Mobile robots,
3. Humanoid robots,
4. Material selection optimization are explained in details.

In the third chapter "*Material and Method*",

1. General system architecture and the functions are explained,
2. The mechanical design and the components of the robotic system are presented,
3. Motion calculations and analyses are presented,
4. Strength check of the components are explained,
5. Modelling of system for numerical analyzes are explained,

In the fourth chapter "*Results and Discussion*",

1. Numerical and analytical calculations are explained
2. Results of tests and material selection criterions and limitations discussed.

2. LITERATURE REVIEW

Robotics have been developed by human capabilities. With the industrial revolution, importance of robotic increased because of maximizing the operations of manufacturing tasks and minimizing the manufacturing costs in the factories. The expectation of robotic instruments development has raised in time and functionality and features of robot usage (construction, firefighting, cleaning, transportation, rehabilitation etc.) have been progressed to provide the human desires.

In a broad sense, robots are categorized as manipulators, mobile systems and humanoid robots. (Garcia et. al., 2007).

The first usage of word “Robota” has been seen in Rossum’s Universal Robots (R.U.R.) play, which was written by the Czech playwright Karel Capek in 1921. The word of “Robota” comes from Slavic Language and means that monotonous work or slave labor. However, the word of “Robot” had partially different meaning in that play. After robots serviced their possessors for a while, the robots rebelled against and also ruined all the life. According to the fiction, the robots had outstanding abilities. Because of Rossum’s Universal Robots play, people began to think about robots in negative way (Wallen, 2008).

Besides Karel Capek, Russian author “Isaac Asimov” used word of “Robot” in his novel, “I’m Robot”. In this science fiction novel, Asimov formulated three fundamental laws for robots. After first publication of the novel, he added the zeroth law. The point of view for robots was in positive manner. Robots were depicted as mechanical creature (automaton) in human look without emotion, intelligence and feeling (Wallen, 2008).

Robotic history dates back to the first century BC and Heron is the first that thought about the open the temple doors automatically using the energy from altar fire with a device which convert the steam to rotational movement. Several nations also promoted the robotic history. For instance, Arabic people were concerned on setting in motion the environment for human comfort. In the 1800s, a Swiss watch company launched out a number of automatons (used before the word “robot) like live dolls.

The great inventor “Nicola Tesla” had a focus on industrial applications. He figured out that there was a parallelism between machines and human in respect to

mechanism, sense and control. In compliance with the Tesla, robots are multifaceted integrated and useful systems, not toys (Rosheim, 1994). He worked on pioneering works about robotics with his robot boat. This robot boat was able to be controlled with radio waves by distant. Tesla's robot boat is presented in Figure 2.1.



Figure 2.1 The Robot Boat (A) Patent Drawing (B) Structure (Rosheim, 1994)

2.1. Robot Manipulators

A robot manipulator is a serial chain of rigid limbs and commonly known as robot arm. Robot manipulators performs a task with end effector. The different definitions can be summarized as given below:

According to the Robot Institute of America (Sciavicco and Siciliano, 2005);

“A robotic system is a programmable tool. It is designed to carry parts and elements. It can perform several different tasks.”

The studies and applications of robotics are the interdisciplinary and in the mechanical engineering field, the machine is studied in static and dynamic situations. The robots have been described the spatial motions in mathematic science, designed for tasks with sensor and interface design by electric electronic engineers, programmed to tools for fulfilling the tasks by computer engineers (Wallen., 2008).

The robot manipulator can be categorized in three topics in basic term as following that (Garcia et al., 2007);

1. Calibration of Kinematics
2. Path and Motion Planning
3. Control

Calibration of kinematics is a process to determine accuracy of the current kinematic models. There are four stages for fulfilling kinematic calibration, as following;

1. Mathematical modelling.
2. The measurement the gap between theoretical and real model by sensors.
3. The determination of the robot's end effector position.
4. The implementation.

The motion planning is conducted to finish the task of the robotic system defined before the starting of the task. In the literature, two methods has been performing as in name of implicit and explicit. Implicit method designates the essential dynamic behavior of the robot. Explicit method identifies path between the robot and target.

The **control** confirms the implementation of the plan required for robot's tasks. The control techniques line up Proportional Derivative (PD) to Proportional Integral Derivative (PID) to adaptive control. The force control is also in the action between manipulator and environment, the contact forces of the end effector.

By the 1990s, new applications fields came in existence such as pharmacy, food industry etc. With these new application fields, the necessity of new specifications and research areas showed up for providing industrial robotic applications. Flexibility and artificial intelligence became the main topic of the new research fields. The flexibility provides an adeptness to robot for self-adaption to the product and environment. Artificial intelligence techniques are utilized to ensure understanding to the robot for managing in dynamic environment and uncertainty.

The Unimate is one of the first industrial robotic applications and was manufactured in United States by Unimation Company in 1961, presented in Figure 2.2. In 1954, it was patented by George Devol and transportation machine designed for handling in the factory and first installed in one of the production line of General Motors in 1962 (Karl, 2010).

“Stanford Arm” was designed by Victor Scheinman in 1969 and has a six-axis arm for chasing inconstant paths in three-dimensional spaces. Standford Arm also enhanced the practicality of the robots for versatile applications such as assembly, welding, etc.

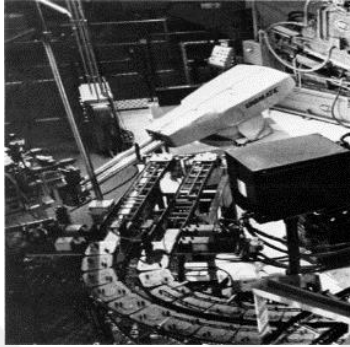


Figure 2.2 Unimate Robot (Karl, 2010)

Japan began to play role in the robotic industry in 1967, after Tokyo Machinery Trading Company began to bring into the Versatran robot from AMF (American Machine and Foundry) Company. After one year, Kawasaki Heavy Industries compromised with Unimation and began to manufacture robot in Japan.

Some statistical information about industrial robots; operational stocks of industrial robots, annual supply of industrial robots according to usage fields and continents are given in figures 2.3, 2.4 and 2.5, respectively (IFR World Robotics, 2018).



Figure 2.3 Operational Stocks of Industrial Robots (IFR World Robotics, 2018).

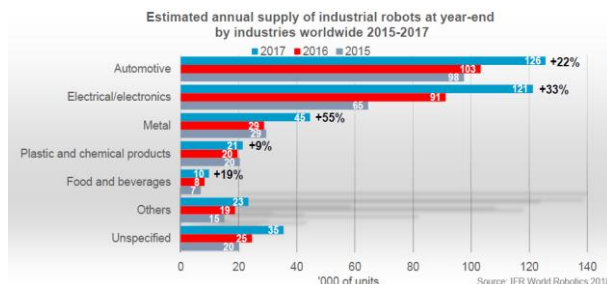


Figure 2.4 Annual Supply of Industrial Robots According To Usage Fields (IFR World Robotics, 2018).

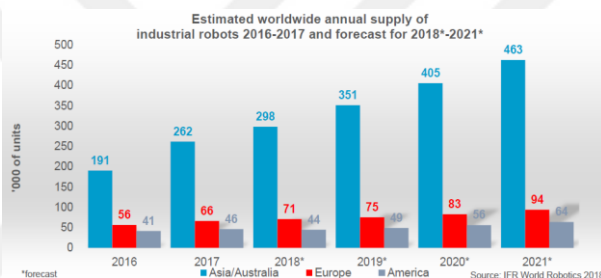


Figure 2.5 Annual Supply of Industrial Robots According To Continents (IFR World Robotics, 2018).

2.2. Mobile Robots

A mobile robot is a system that has ability to move on the ground, on the surface of bodies of water, under water, and on the air. Unlike fixed based industrial robot, a mobile robot has unlimited movements by its size due to its mobility. While fixed based industrial robots are programmed to fulfill repetitive tasks with limited sensors, mobile robots are typically less structured in their operation and likely to use more sensors. Mobile robots can be utilized to perform numerous of tasks which are normally accomplished by humans such as rescue, investigation, disaster response, agriculture, military, explosive disarmament and exploration of other planets, observation, exploration, rounds, fire searching-fighting, homeland security, care taker, demonstrator (Chen et al., 2009; Cook, 2011).

A mobile robot system be composed of locomotion mechanism components. The movement mechanism bases on the environment in which the robot will run. There are three ambient, respectively aerial, aquatic or terrestrial. Mobile robots in different ambient are presented in Figure 2.6.

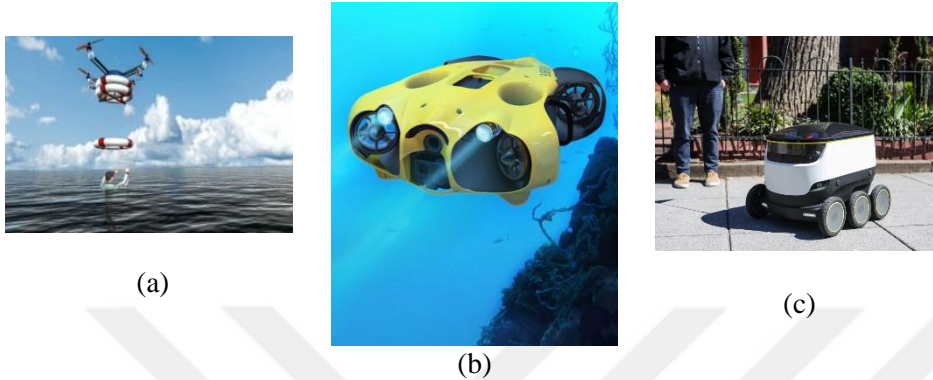


Figure 2.6 Mobile Robot Samples (A) Aerial Rescue Robot (B) Underwater Robot (C) Mobile Delivery Robot (Chen et al., 2009).

Apart from terrestrial environments, the locomotion mechanism generally consists of propellers or screws. The conventional terrestrial locomotion components rank as wheels, tracks and legs.

A system on mobile robotic has a set of similar operational parts with humans. These operational parts comprise of cognitive, actuation, mobility, sensory, communication and energy (Chen et al., 2009). A model is presented in Figure 2.7.

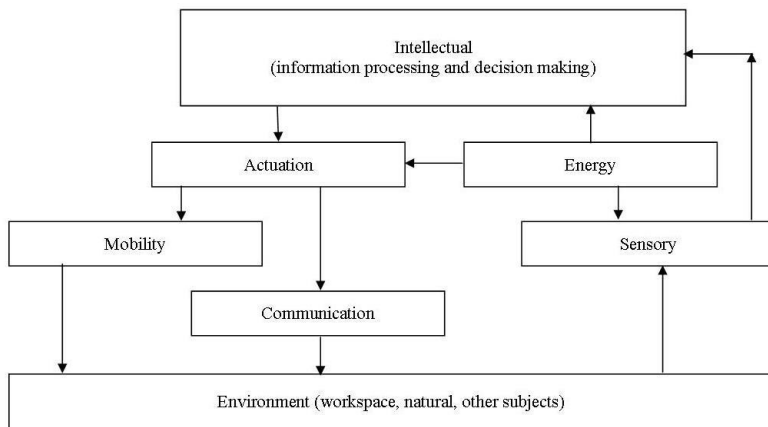


Figure 2.7 Model of Mobile Robot's Functional Parts (Chen et al., 2009).

1. **Cognitive and actuation part;** fulfills check with the actuation part, which provides the motion system with information and decision process.
2. **Energy;** a mobile robot spends energy onto environment and energy conversion occurs such as kinetic energy, mechanical energy, wave energy etc.

3. **Mobility**; there are statue and motivational parts. Statue is the body and mechanical frame of the robot. Motivational part provides enlargement or refinement of the robot mobility for executing the particular tasks. These parts react with the environment, during a mobile robot performs its duty. This operating environment can be sorted out in three types;
 - a) Pre-defined and structured environment, the robot have knowledge about the working environment. It subsists in the plant automation.
 - b) Semi structured environment, the robot knows the environment, yet the conditions can be changed spatially and temporally.
 - c) Unstructured environment, the robot (for example underwater robot) may not have information about the environment. Its sensory and navigation system becomes involved.
4. **Sensory**; during the mobile robot applies its duty; it communicates with the environment via video, image or data. The robot utilizes sensor for getting the desired information.
5. **Communication**; this part is indispensable for most mobile robot applications. With this function, it can be provided some tasks such as monitoring the robot, communication with other robots or environments.

An analogy of human beings and mobile robot is given in Table 2.1 (Chen et al., 2009).

Table 2.1 Comparison of Robotic System and People by the means of Properties

Functionality	Human Parts	Robotics
Cognitive	Brain	Microprocessor
Statue	Skeleton	Mechanical frame (airframe, chassis, hull)
Motivational	Legs	Tracking systems
Actuation	Muscles	Different types of actuators
Sense	Receptor	Sensors
Communication	Speech, gesture	Data acquisition
Energy Source	Food	Power source / energy storage

Mobile robot can be designed under three main topics;

1. Software
2. Hardware
3. Mechanical

The software development is mentioned into high-level software and low-level software.

- High-level software is to perform its assignment and function autonomously.
- Low-level software involves the main motor functions such as collision avoidance, etc.

The hardware design comprises of electronic parts, actuators and sensors.

- Electronic parts are used to convert the software requirements into actuator control signal and calculate, digitize the signals.
- Actuators ensure converting the signal to the motion.
- Sensors collect the data from the environment and transform them into signal for locomotion and monitoring.

The mechanical design consists of mechanisms and body design.

- Mechanisms are used to be turned into the actuator's motion.
- The body design ensures to preserve the robot from environment and it provides integrity to mobile system.

The former mobile robots were mostly designed as AGVs (automated guided vehicles) that generally used to carry the equipment in defined path. The current mobile robot studies and applications are designed with autonomous manner. The mobile robot research topics consist of four components (Garcia et al., 2007):

1. Perception
2. Localization
3. Path and Motion Planning
4. Generation of Motion

The terms of perception and cognition usually replace with each other. However, in robotics, cognition means the formation of the high-level and low-level information. High-level information can be employed on the mapping and prediction of environment. Patranik (2007) propounded a model of cognition that consists of seven mental states as reasoning, attention, recognition, sensing and acquisition, learning, planning, coordination and action.

In settled environments, perception permits mobile robot to come up with models and maps for path and motion planning and generation. Yet, in the dynamic environments, the robot has to come to know to navigate. So researches in mobile robotics focuses on mapping and localization (Garcia et al., 2007).

A mobile robot can know where it is relative to its environment at any moment, with allowing self-localization. With this objective, numerous types of sensors can be used for estimations of robot's state and environment. The localization can be local or global.

Robot mapping is a technique for enabling a mobile robot to construct and maintain a model of its environment based on spatial information gathered over time (Wallgürn, 2010). Robot mapping comprises three steps (Valgren, 2007):

1. Map Learning
2. Localization
3. Motion and Path Planning

According to if or not the robot has a map, localization and mapping will be easy. When the robot knows its position, robotic mapping is referred to as Simultaneous Localization and Mapping (SLAM) (Hahnel et al., 2003).

The market of mobile robots has been enlarging for several years. Especially service and military mobile robots are the most common and developed types. Service mobile robots are divided into as professional and domestic mobile robots. In recent years, delivery mobile robots (professional mobile robots) have been increasingly popular for logistic companies, due to employ transportation and delivery goods for costumers in low cost and short time periods. Another example is that medical robots can be used as assistant or trainer for surgeries. The domestic robot type includes educational, home care, entertainment applications. (Chen et al., 2009).

The evolution history of mobile robot as ground vehicles began with the Grey Walter's tortoises. He firstly developed two robots between 1948 and 1949; Machina Speculatrix presented in Figure 2.8. Those robots had ability to find their way for charging with three-wheeled (Arkin, 1998).

Shakey was one of the first mobile robots with intelligence and was constructed in SRI in 1968, presented in Figure 2.9. It had a TV camera, range finder and bump

sensors. Shakey was programed for perception, world modelling and acting (Arkin, 1998).

The Stanford Cart was designed as a line follower in 1970. In 1979, it was rebuilt and equipped with 3D vision system by Hans Morevac, presented in Figure 2.10. According to experiment of Stanford Card, it crossed a chair-filled room autonomously via TV camera, which was taking picture from several angle. Those pictures provided to avoid obstacles (Nehmzow, 2003).

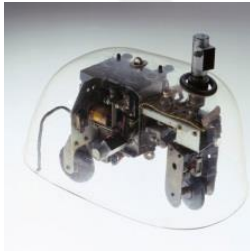


Figure 2.8 Grey Walter's Turtle (Arkin, 1998).



Figure 2.9 Shakey Robot (Arkin, 1998).



Figure 2.10 Stanford Cart (Nehmzow, 2003).

A robotic research group from MIT (Massachusetts Institute of Technology) developed Genghis Khan mobile robot in 1988, presented in Figure 2.11. Genghis Khan was designed with 6 legs, 12 motors, 12 force sensors and 6 pyro electric sensors. Genghis Khan could learn how to scramble over boards and other obstacles (Brooks and Flynn, 1989).

The Khepera robot was developed by Nicoud in 1994 in Switzerland, presented in Figure 2.12. This miniature robot had a circular shape and dimensions as 55 mm diameter and 30 mm height. In its system, it had eight infrared proximity sensors for proximity and obstacle avoidance sensor (Lund and Miglino, 1996).

Stanley was designed as an autonomous car that won the 2005 Darpa Grand Challenge, presented in Figure 2.13. This robot was built with laser range finder, GPS system, six DoF inertial measurement unit and wheel speed measurement unit for pose estimation (Thrun et al., 2006).

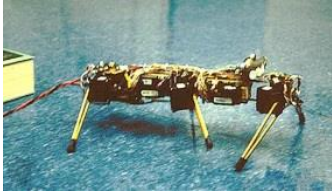


Figure 2.11 Genghis Khan Robot (Brooks and Flynn, 1989).



Figure 2.12 Khepera Robot (Lund and Miglino, 1996).



Figure 2.13 Stanley (Thrun et al., 2006).

According to utilization are, there are several examples of mobile robots. In order to explore Martian soil (Figure 2.14), the first robot was used in the Pathfinder mission in 1997. It was practically only operated from hearth. It had front and rear cameras at the front and rear and hardware to conduct several scientific experiments. The main purpose of this vehicle was to determine the composition of Martian soil.

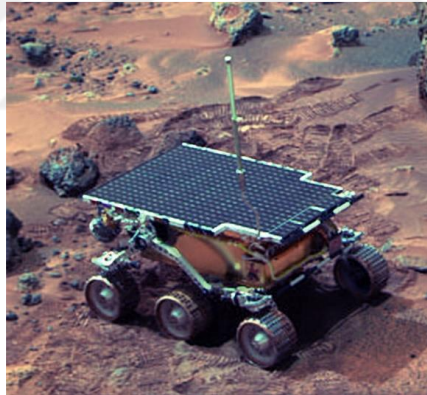


Figure 2.14 Sojourner or Rover (Mars Rover, 2019).

Skid Steer robots are used in many different application due to its robust structure and adaptability. Boston Dynamics are researched a robotic system (Figure 2.15) which have ability to jump when it is required and to move linear on the ground.



Figure 2.15 SandFlea (Boston Dynamics, 2019).

NASA has developed a robotic system which has capability to obtain the samples from required environment. It is especially designed with the responsibility of Chernobyl disaster, presented in Figure 2.16.



Figure 2.16 Pioneer (Nasa, 2019).

Many different robotic systems have been developed for agriculture usage. Two different samples from them are presented in Figure 2.17. They are multipurpose robotic systems. They have for wheels, which can drive steerable. They have also high motion capability.



(a) (b)
 Figure 2.17 Mobile Robots Used In Agriculture: a) Bonirob Developed By BOSCH Deepfield-Robotics (Bosh, 2019), b) Thorvald was Designed By SAGA ROBOTICS (Saga Robotics, 2019).

For the mine usage, different type of robots have been developed. One sample of them is presented in Figure 2.18 (Marques et al., 2012; Rodriques, 2017).



Figure 2.18 Husky with Mechanisms That Make Him Prepared To Detect Mines (Cabrita Et Al., 2015).

Statistical findings and estimation about mobile service robots; sales for professional usage between 2016 and 2018, sales forecast for professional usage between 2019 and 2021 and sales for domestic usage are given in respectively Figure 2.19 and Figure 2.20 (IFR World Robotics, 2018).

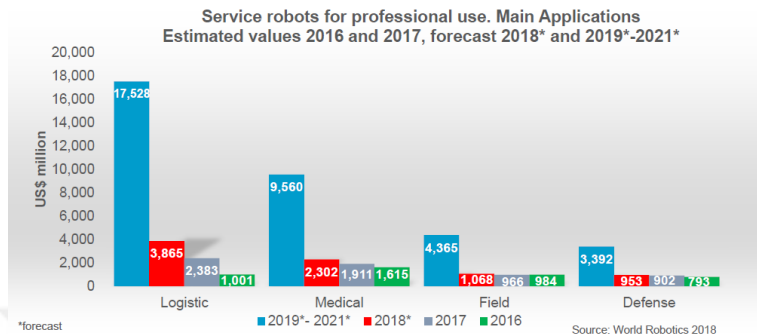


Figure 2.19 Mobile Service Robots Sales for Professional Usage And Forecast Between 2016-2021 (IFR World Robotics, 2018)

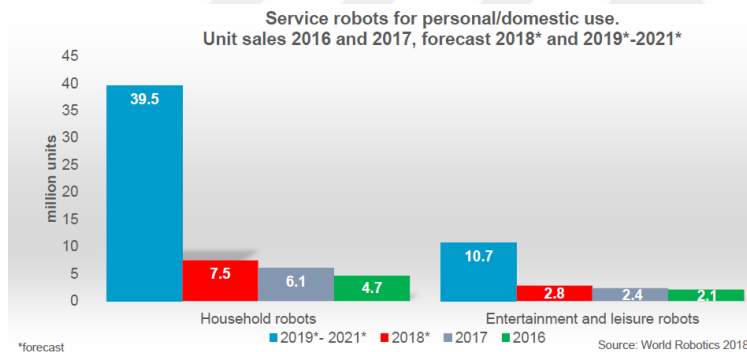


Figure 2.20 Mobile Service Robots Sales for Domestic Usage (IFR World Robotics, 2018)

2.3. Humanoid Robots

Beyond the conventional mobile robots, of which locomotion mechanism has wheels or tracks, biologically inspired robots are manufactured with customizable locomotion mechanism. The leg is the most extensive locomotion mechanism for biologically inspired robot. The limbs or legs can be provide walking on a hard or soft surface (Ceccarelli and Carbone, 2005).

The legged mobile robots have two or three DoF manipulators. Comparing with the other types of mobile robots, legged mobile robots have some advantages and disadvantages (Garcia et al., 2007).

Despite the fact that legged mobile robots have advantages, legs have a number of challenges in their own. Legged mobile robot researches are concentrated on leg movement and coordination over the course of robot navigation. As long as the legged mobile robot is able to keep its balance, it will be stable.

The static stability was originated from insects. It was supposed the lack of inertia in the motion of the robot limbs. Nevertheless, while the robot limb motion, it was found some inertial impacts and other dynamic components deriving limited robot movement. Thus, researchers started to focus on dynamic stability. M. Raibert (1986) developed the first dynamic stable system in the MIT. Till this development, many researchers concentrated on statically stable multi-legged systems in order to develop dynamically stable robots (Santos et al., 2006). Raibert studied on machines with more than one leg to solve one leg problem and ultimately, he achieved. Sketch drawing of his system is presented in Figure 2.21.

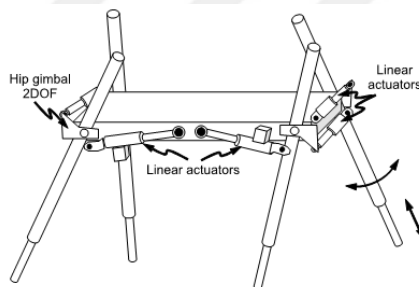


Figure 2.21 The First Dynamically Settled System (Santos et al., 2006)

Walking gait is forth application field for mobile robots and it is related to the stability. Leg is a component of locomotion mechanism that discontinuously get in touch with the ground, it is significant to decide the types of gait and the sequences of leg movements (Garcia et al., 2007). According to stability criterion, two gaits can be mentioned:

1. Statically settled gait (Figure 2.22-a)
2. Dynamically settled gait (Figure 2.22-b)

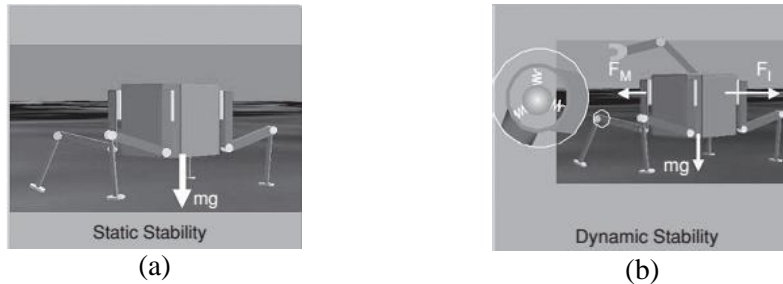


Figure 2.22 Gait Types (A) Statically Settled Gait (B) Dynamically Settled Gait (Garcia et al., 2007)

Statically settled gaits have the feature of making simple the control of the robot with heavy limbs. They can be sorted as periodic and aperiodic gaits. Periodic gaits comprise of predefined series of motions that are replicated cyclically. Aperiodic gaits are more flexible for non-uniform terrain.

Due to the necessity of being faster than wheeled or tracked robots, legged mobile systems are in dynamically needs of settled gaits. The dynamically settled gaits have been enhanced up to now are limited with the trot, the pace and bound movements.

In the mythology and ancient scripts from Greek, Indian, Egyptian and Chinese civilization, it has been referred to the concern about understanding techniques of legged locomotion in the nature and the exertions for replicating them to mobilize (Zielinska, 2004; Nonami et al , 2014),

At the fifteenth century, the first ideas about fulfilling the legged locomotion for vehicles began to show up. The first articulated anthropomorphic robot in the history of western civilization between 1495 and 1497 was designed and built from Leonardo Da Vinci. His knight in the armor could sit up, wave it arms and move its head, presented in Figure 2.23 (Silva and Machado, 2007).



Figure 2.23 Knight In the Armor and Its Inner Mechanism (Silva and Machado, 2007)

L.A. Rygg suggested the first quadruped machine named as The Mechanical Horse in 1893, presented in Figure 2.24. This design was patented and had stirrups as pedals. The rider was able to power the mechanism. The motion from pedals was transmitted to legs through gears. However, it is not certain that this machine actually built (Nonami et al., 2014).

Georges Moore suggested a biped machine, named as Steam Man, in 1893, presented in Figure 2.25. It was driven by 0.5 hp boiler and reached the speed 14 km/h. A swing arm was employed for stability. A pressure gauge was transported to its neck (Silva and Machado, 2007).

A quadruped machine was designed and patented a quadruped machine in 1913 by Bechtolsheim Baron, yet there is no proof that this machine existed (Silva and Machado, 2007).

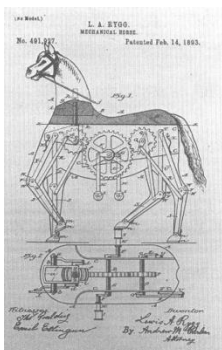


Figure 2.24 Mechanical Horse (Nonami et al., 2014)



Figure 2.25 Steam Man (Silva and Machado, 2007)

After World War II, mobile robot research accelerated because of new inventions in material science, electronics, electronics, computers and control systems. Most

of researchers began to work and enhance modern systematic walking machines with new approaches in 1950s (Garcia et al., 2007).

Ralp Mosher designed a four-legged truck, referred as General Electric quadruped, presented in Figure 2.26. It was begun and finished between mid 1960s and 1968. Its legs had three DoF; in knee and two in the hip. A crank with hydraulic cylinder energized each DoF. The dimensions were 3.3 m height, 3 m long and 1,400 kg weight. A 68 Kw internal combustion engine activated it. Well-trained operators controlled General Electric quadruped with four joysticks. In spite of the control severity, this design was so substantial for the modern mobile robots. It had ability to outrival the obstacles in difficult terrains (Kar, 2003).

McGhee and Frank developed walking robot Phony Pony in 1966, presented in Figure 2.27 (Reeve and Hallamr, 2005). It was the first fully computer controlled walking robot. Its each leg had two DoF. The modern digital computer performed via joint coordination. A worm gear speed reduction system triggered joints via electric motors. Phony Pony had externally power supplier as a cable. It could move with two different gaits; the first one was quadruped walk and second was trot (Nonami et al., 2014).

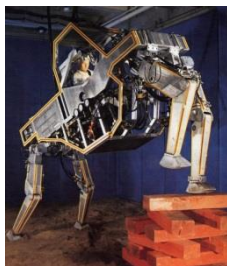


Figure 2.26 General Electric Quadruped (Kar, 2003)

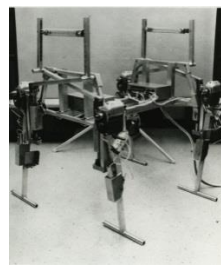


Figure 2.27 Phony Pony (Reeve and Hallamr, 2005)

Big Muskie was developed by Bucyrus-Erie Company in 1969, presented in Figure 2.28. It utilized for open-air coalmine. The biggest off-road walking machine is Big Muskie with weight about 15,000 tons up to now. Big Muskie had four hydraulically actuated legs. Its body could move forward backward and then lower on the ground. The legs could lift and move the machine for next position, when the body was on the ground. Electronic sequencer revolved for the motion (Silva and Machado, 2007).

McGee and his research team from Ohio State University built the OSU Hexapod, presented Figure 2.29. It was an empirical study for terrain adaptability, man-machine interaction and locomotion. There were three joints, which had individual motors. In order to feedback joint angle and joint rate information, every joint was equipped with one potentiometer and one tachometer. OSU Hexapod had also gyroscope, a camera system, force sensors and proximity sensors. A PDP-11/70 computer was utilized to ensure the computational power to robot for real time control (Ozguner and Tsai, 1985).



Figure 2.28 The Big Muskie (Silva and Machado, 2007)

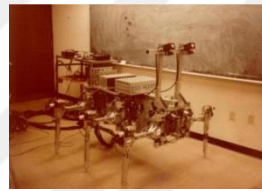


Figure 2.29 OSU Hexapod (Ozguner and Tsai, 1985)

PV-II was developed as a four-legged walking robot by Hirose and Umetani in Tokyo Institute of Technology in 1980, presented in Figure 2.30-(a). PY-II was 10 kg and had very low speed only 0.02 meter per second and 10 W power supply. DC motors and power screw speed reduction system carried out the leg actuation. It was provided to maintain a horizontal body orientation with its control system. There were contact sensors on every foot to realize obstacles on the route (Nonami et al., 2014).

PV-II achieved climbing the stairs grounded on sensor. This sensor worked according to motion control system. Also it had the tactile and attitude sensors for the first time. Moreover, Aruku Norimono designed the TITAN-III as the larger version of the PV-II in 1984 in Tokyo Institute of Technology, presented in Figure 2.30-(b). It had intelligent program to create applicable motion in terrain. It had 1.2 m length of leg and 80 kg. It was used composite material on its design (Hirose and Kato, 2000). TITAN-XI was built in 2008 as the latest TITAN series robot. This hydraulic quadruped robot was 7,000 kg. It was developed for drilling holes to reinforce steep slopes with rock.

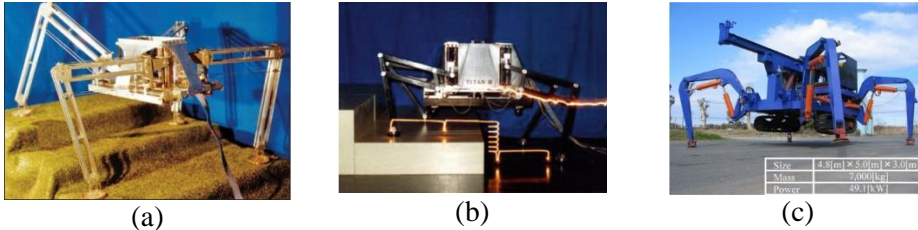


Figure 2.30 Tokyo Institute of Technology Robot Series (a) PV-II (b) TITAN-III (c) TITAN-XI (Nonami et al., 2014)

The primary difficulties for the development of autonomous mobile robot can be summed up as (Nonami et al., 2014);

1. There is no availability of energy efficient actuators.
2. There are reliable and economical sensors,
3. They are lighter comparing with the other types of robots, yet they have mechanically strength materials for structure and mechanism,
4. They have computers with faster and higher computing power,
5. Their power source is usually light and integrated for long duration energy.

Present autonomous biped (humanoid robot first put in appearance with dermato-skeletons experiment in 1967 by Vukobratovic et al. (Garcia et al., 2007). WABOT- 1 was the first robot that had controller based full-scale anthropomorphic and made in Waseda University in 1973 by Kato et al. It had ability to correspond with a human in Japanese. It had external receptors for measurement between the distance, direction of the objects. WABOT-1 could hold and carry the objects via its hands by means of tactile sensors (Lim and Takanishi, 2006).

WABOT-2 was developed by Kato et al. and da ability to play an electronic organ and read the music, presented in Figure 2.31-(b). There were wire-driven arms and a hierarchical system of 80 microprocessors. It had 50 DoF of its leg (Behnke, 2008).

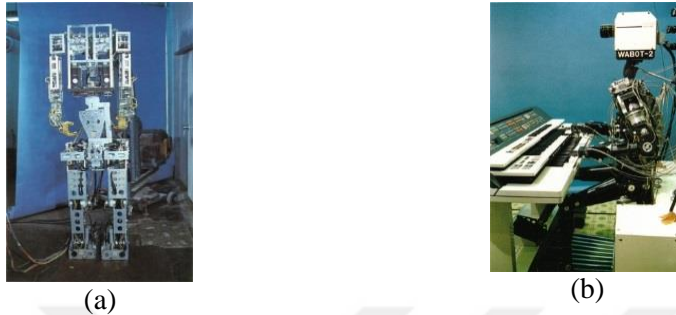


Figure 2.31 Waseda Robot Series (a) WABOT-1 (b) WABOT-2 (Lim and Takanishi, 2006)

After in 1986 Honda started ASIMO Robot Project, Honda introduced first product P2 robot in 1996, presented in Figure 2.32-(a). This humanoid robot has self-contained full body for the first time. P2 had no ability not only move on the flat ground but also climb the stairs. P3 followed P2 robot in 1997, presented in Figure 2.32-(b). In the latest of 2002 ASIMO robot was developed, presented in Figure 2.32-(c). It had 34 DoF, 54 kg weights and 130 cm total height. ASIMO had ability to pace and run in smooth or orbicular paths, climb up or down the stairs and perform intuition such as localization, tracking, recognition, localization, identification and obstacle avoidance (Behnke, 2008; Duran and Thill, 2012).

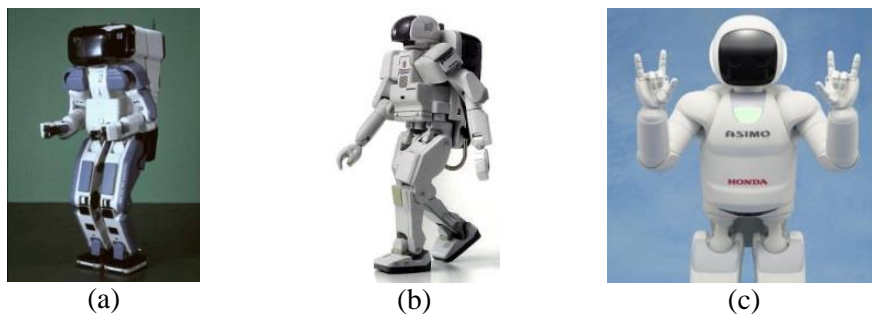


Figure 2.32 Honda Robot Series (a) P2 (b) P3 (c) Asimo (Behnke, 2008; Duran and Thill, 2012)

Another significant turning point of the humanoid robot evolution was actualized. Sony Company introduced the Qrio, Sony Dream Robot, in 2000. This robot could dance and walk like human beings, because it was a fully dynamic humanoid robot. It could also identified the faces, reveal body movement like mimic and some emotions (Geppert, 2014).

This robot studies can be summed up in topics as below (Garcia et al., 2007; Behnke, 2008);

1. Two-legged locomotion
2. Representation and perception of emotion
3. Mutual effect between human-robot
4. Skillfully manipulation
5. Learning and adaptive ability

For two-legged locomotion, there are two common attitudes. The first is ZMP (Zero Moment Point) theory introduced by Vukobratovic. According to theory, there is a point on the ground and called as ZMP. The sum of the moments of all active forces equal to zero. No sooner than the ZMP is in the support polygon of all contact points between the feet and ground, the humanoid robot will be dynamically immobile (Vukobratovic and Borovac, 2004). Honda ASIMO and Sony Orio are the leading robots and depend upon ZMP based control (Behnke, 2008). The version of 2006 ASIMO could run with 6 km/h speed with ZMP based control. However, its gait did not look like a human being. ASIMO wasn't able to store the energy in elastic elements. Moreover, it had ability to climb certain stairs.

Utilizing robot dynamics is the second approach. McGeer showed that the chance of the walking down a slope without actuators and control in 1990. He maintained his research on two elementary passive mobile models from a wagon wheel. These models are presented in Figure 2.33 (Narukawa et al., 2010).

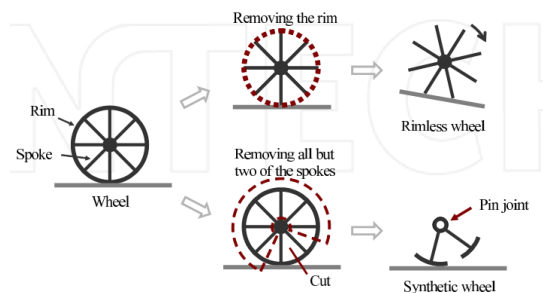


Figure 2.33 Two Passive Mobile Models of Mcgeer (Narukawa et al., 2010)

McGeer showed that the edgeless wheel has a periodic motion and in the first model, it was very large. The edgeless wheel will never falls forward, unless the initial rolling speed and slope angle are adequate. This feature can strengthen the stability

of passive walkers. A pin joint and a large point mass were put at the hub at the artificial model. When comparing the hub mass, If the leg mass is accepted to be negligible, the swing leg motion doesn't disturb the stance leg motion. On the floor and at a constant speed, the stance leg rolls, since it is as part of the wheel. McGeer made the biped model complex and developed various physical walkers with or without knees, presented in Figure 2.34 (Hobbelen and Wisse, 2007).

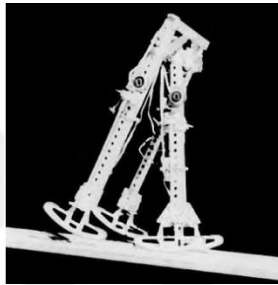


Figure 2.34 McGeer's Straight Passive Dynamic Walker (Hobbelen and Wisse, 2007)

The studies, mentioned before, have been used for functional given fillip to two-legged and passive dynamic motion and then machines have been built.

The successful act of humanoid robot depends on perception of its own and environmental states. Using encoders, force sensors and potentiometer support measuring the state of their joints for proprioception. The estimation of robot attitude is important for balance and it can happen with accelerometers and gyroscopes (Behnke, 2008). Numerous humanoid robots can measure the forces of the ground at their hands and fingers, because they have force sensitive skin.

CB² was developed in Osaka University by Takashi et.al, presented in Figure 2.35. This humanoid robot is similar with a child boy in size and about 130 cm high, 33 kg weights (Minato et al., 2007). Its body is covered with soft silicon skin and many tactile sensors.

Vision and audition are the most important method for the perception; however, some humanoid robots have superior human senses such as laser range finder, ultrasonic distance sensors (Behnke, 2008). In general, transportable and attached stereo cameras and on-board computers are performed for vision perception. Besides, a real-world image sequence is not a solved problem. In simplistic environment, these systems can only work. For sound perception, on-board

microphones are performed. The main problem is the separation of concern sound source from other sound sources and noise. Tele operation systems have been developed for described difficulties in perception. In such systems, robot caught signals and construed with human. Gemiboid robot was developed by Ishiguro et al. and is a representative for tele operation systems, presented in Figure 2.36. This humanoid robot looks and acts like a person. It can be controlled with an autonomous program and manual. The limitations in introducing the manual control can be avoided for perception and long term intelligent human-robot interactions are enabled (Nishio et al., 2007).



Figure 2.35 CB² Robot (Minato et al., 2007)



Figure 2.36 Geminoid Robot (Nishio et al., 2007)

The human-machine interaction is evolved from human-human interaction. This interactions comprises modalities such as speech, eye gaze, gestures, body language etc. For accomplishing thee modalities, interaction ability of humanoid robots has expressive animated heads (Behnke, 2008).

Kismet is the one of the example and developed in MIT, presented in Figure 2.37- (a). Kismet is sociable robot fir the first time in the world. Kismet can get eye contact with people. Its mood can be read from speech. It can communicate with gestures (Richardson, 2008).

Robots with anthropomorphic features can be utilized for creating gestures. These created gestures of humanoid robots comprise waving, greeting and pointing. Its head can point and shake (Behnke, 2008).

Hubo robot, developed in KAIST (Korea Institute of Science and Technology), had articulated fingers. Due to this feature, robots can communicate with sign language, presented in Figure 2.37 (b). Hubo robot had about 125 cm height and 55kg weight.

It could take the human motions off such as hand shaking, bowing and walking. Hubo could move its fingers and eyeballs separately. It had two DoF for each eye as camera pan and tilt, seven DoF for each hand and one DoF for each finger (Park et al., 2005).

The farthermost a humanoid android was developed in Osaka, named as Repliee Q2, presented in Figure 2.37-(c). It was form of communication humanoid robot. It looked like a Japanese woman and had a kind of silicone-covered skin. Repliee Q2 could create a great number of motions and gestures (Matsui et al., 2005).

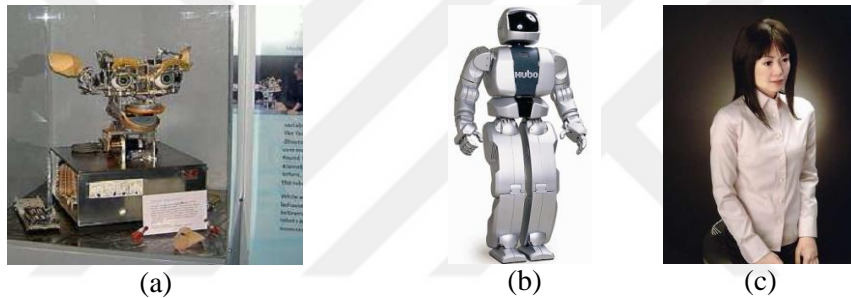


Figure 2.37 Humanoid Robots (a) Kismet (b) Hubo (c) Repliee Q2 (Park et al., 2005)

Shadow Robotic Company developed Shadow and it has advanced robotic hands. There are position and force sensors, 40 air muscles and sensitive tactile sensors on its fingertips (Shadow Robot Company, 2019).

Humanoid robot can come to know new skills and adapt with expedition. On the contrary of statistical learning approaches, latest techniques assist robots to gain new skills and tasks (Breazeal et al., 2006).

Between 1960s and 2005, the time evolution of the robotics studies are presented in Figure 2.38 (Garcia et al., 2007).

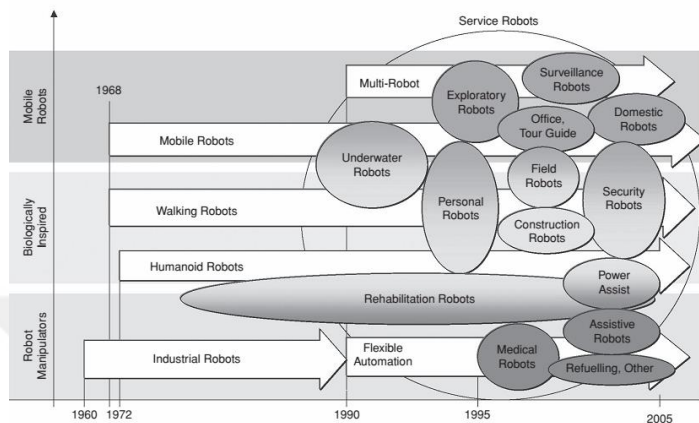


Figure 2.38 Time evolution of The Robotics Studies (Garcia et al., 2007)

2.4. Material Selection

2.4.1. Material Selection Process

For all engineers, the material selection is a process, beginning with the identifying the desired attributes of engineering problem. The main design requirements is significant to fit the targets of the problem such as maximizing the strength of material and minimizing the cost of material. Determining the requirements and attributes is the important thing so that adequate material can be matched. In this step, all materials are considered as possible options for engineering problem.

The process of material selection is consisted of four main steps as below:

1. **Translation:** It is the process of determination of design requirements.
2. **Screening:** It is the process of definition of the constraints.
3. **Ranking:** It is a sorting process according to suitability to the requirements.
4. **Supporting:** It is a step to find and to use the support information such as mechanical strength, mechanical properties (Ashby, 2011).

2.4.2. Material of Robot Frame

After deciding what kind of robot is designed, next steps are following as construction, material selection etc. In material selection, there are numerous option to use for building robot. Likewise, traditional materials can be used; raw materials

such as plywood or sheet metal, various creative materials such as inexpensive house wares or toys can be used. However, in this point some features may be limited according to mechanic design properties of robot.

Robotic frames are commonly produced using four types of different materials. These materials are plastic, wooden, metal and composites. These materials are selected according to different properties as listed below:

- Size
- Cost
- Function
- Weight

The robotic systems are also designed with different body shapes such as;

- Oval
- Square
- Round
- Other specific shapes

The first material is wooden. It is generally selected as robot chassis material due to low-level of price. Commonly used wooden types are listed below:

- Oak
- Pine
- Fir
- Ash
- Birch

Plastic type is the second. Injection moulding and additive manufacturing technique are generally used for robotic chassis manufacturing. The most common plastics used for robotic chassis are listed below:

- Polycarbonate
- Acrylic
- PVC (Poli Vinil Clorür)
- Liquid urethane resin
- PLA

- ABS

Metals are used as another robotic chassis material. Although metal chassis is more expensive than the previous materials. They are selected due to their high mechanical strength. These metals can be selected as steel or aluminum. Aluminum is more suitable one as its softer and easy to manufacture (Robotic Universe, 2019).

Composite frames can include laminated material, fiberglass and resin, and carbon or graphite materials. The laminated material generally combines wood, paper, plastic, or metal to allow the best properties. A common laminate material would be foam. For fiberglass and resin, filler materials such as metals or carbon are added in order to increase the strength of the material. The final composites include carbon and graphite, which increase the strength (Pavlak, 2016).

3. MATERIAL AND METHOD

In this thesis, an adaptive robot for multi purposed tasks that requires to climb over the obstacles and ladders was designed. Adjustable motion system that can behave as both legged and wheeled robot utilizing from transitional gear system with three-wheel.

System was considered to work as legged robot with activation of main gear using designed linear actuation mechanism. This activation converts rotational motion to linear motion and pushes main gear to lock in gear channel in outer cover and actuates as legged locomotion system. Deactivation of linear actuation mechanism pulls main gear from gear channel and connects gear system to transfer actuation from main gear to wheels and transforms robots actuation system to wheeled system.

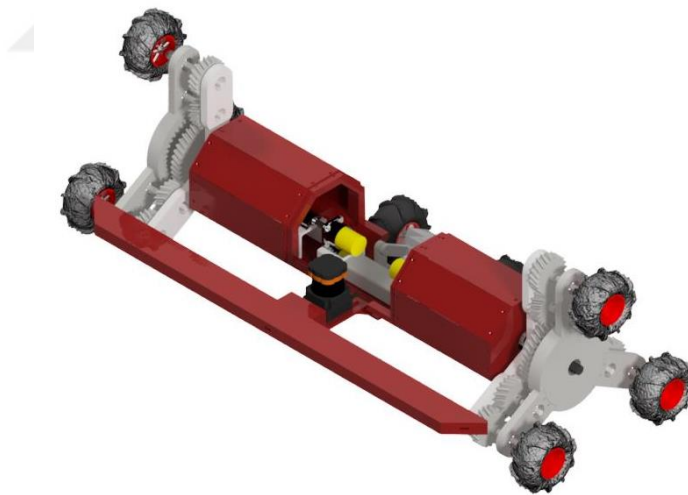


Figure 3.1 The Developed Robotic System

The aim of this thesis study are listed as below;

1. Design a transitional mechanism for legged and wheeled robot.
2. Design durable and material effective robot structure considering suitability for both additive manufacturing and machining.
3. Determine nominal and extreme load for straight road and climb over obstacle conditions.
4. Specifying optimum material for extreme conditions.

According to the aim of thesis study the design goals and criteria are listed as;

1. Robot structure and locomotion mechanism should be robust and designed to withstand both straight road and climb over conditions.
2. Drive-Train of locomotion system should be calculated and verified.
3. Optimum material in the mean of lightweight should be selected according to results of verification.

3.1. Design of Drive-Train for Transitional Locomotion Mechanism

In the design process, firstly ladder/obstacle dimensions were specified and mechanism concept were created using parametric CAD software Autodesk Inventor. Then, conceptual dimensions were transformed to solid parts that can be manufactured using additive manufacturing and machining.

In the design stage of transitional locomotion mechanism, several criteria were taken considered as:

1. Designed system must be easy to assemble and disassemble.
2. Concept ladder and obstacle must be climbable.
3. Tolerances of the components must be considered for assembly and manufacturing process.
4. Commercial equipments must be easy to get and withstand loads.

Drive-train of ladder climbing robot was designed considering specified and wheel dimensions were used to proceed in conceptual design. Ladder dimensions were given in Figure 3.2.

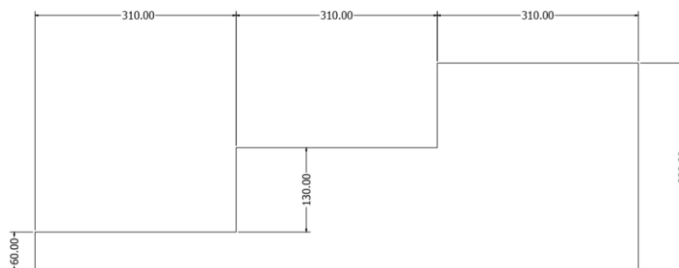


Figure 3.2 Ladder/Obstacle Dimensions in mm

Specified ladder dimensions had crucial importance for design system to define maximum dimensions for robot to operate without failure.

Height and center of the robot were important parameters to succeed in climbing process. In conceptual design, wheel dimensions were required to be defined and selected. In the beginning, Pololu off-road type of wheels were selected for several reasons such as, roadholding, price/performance ratio and easy-to-get from market with diameter about 120 mm and width of 60 mm (Figure 3.3).



Figure 3.3 Off-Road Type Wheels (Pololu)

Specified dimension parameters of ladder and wheel were used in block based template to simulate robot rotation over obstacle. In template, free body diagram for wheel, leg and tail connection and climbing rotation were simulated manually (Figure 3.4).

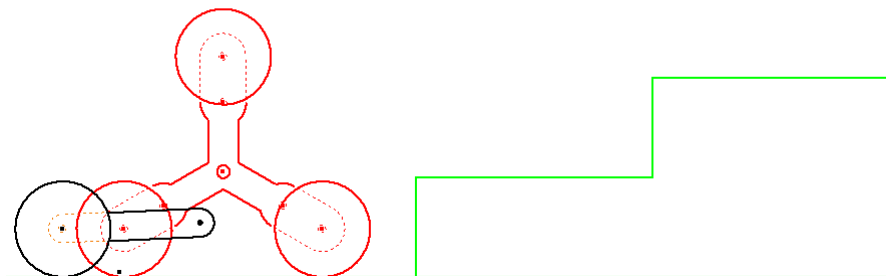


Figure 3.4 Initial Position of Ladder Climbing Mechanism

In block based template, each block was highlighted with different colors to understand mechanism basically. For this representation, colors are meanings are;

- Red : Drive-Train Mechanism
- Black : Supporter Tail
- Green : Platform and Ladder
- Blue Arrow : Axes of Rotation

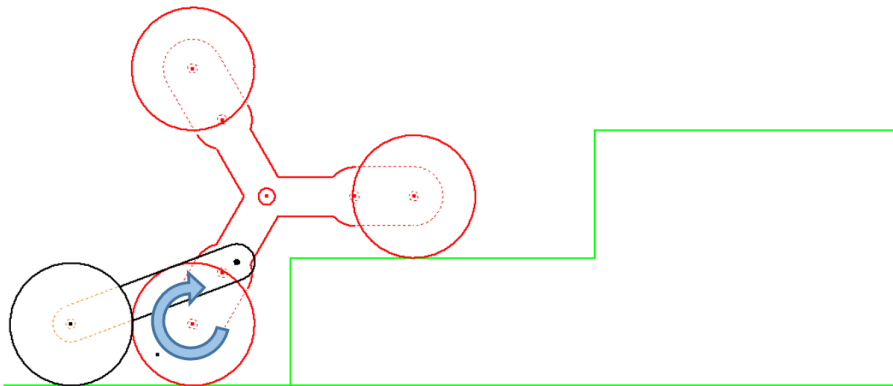


Figure 3.5 Climbing Position

Block based template was used to specify leg length, diameter of rotation circle and maximum distance from center of mechanism to ladder to carry out climbing motion. Also, this template is used to specify chassis dimensions that avoid to strike to corner of the ladder.

After determination of leg length and testifying rotation of mechanism, gear modules and number of teeth that will satisfy center distances in legs and rotation of wheels according to the robot were determined. Transmission of robotic system is consist of seven gears as three inner gear, three outer gear and main gear.

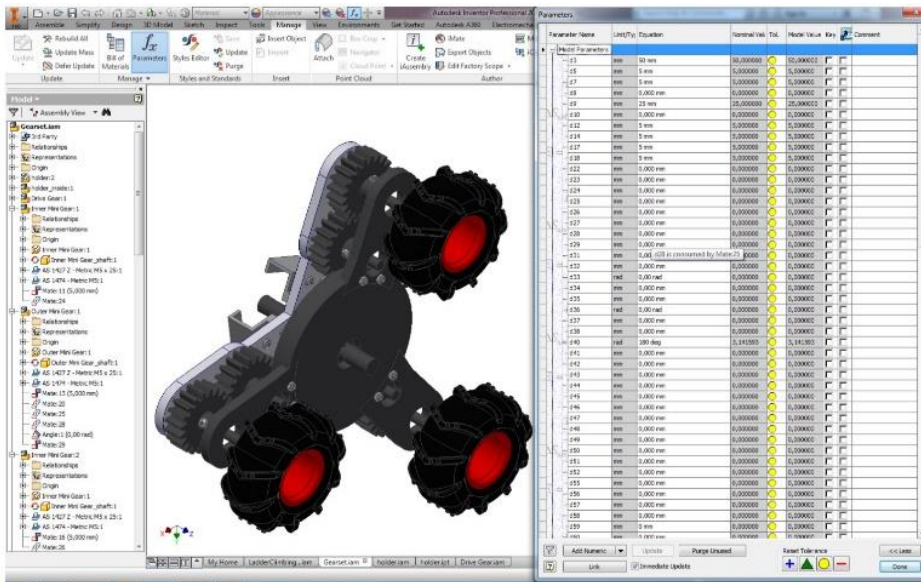


Figure 3.6 Transmission System of Robotic System with Parameters

Utilizing the block based template and designed system structure, modules and number of teeth of gears were defined. General information for gears were given in Table 3.1 with general technical drawings of gears (Figure 3.7).

Table 3.1 The Dimensions of the Gears

			Main Gear	Outer Gear
Symbol	Parameter and Unit	Equation	Value	
m_n	Normal module, mm	$m = p/\pi$	3	3
m_a	Face module, mm	$m_a = m_n/\cos\beta$	3.19	3.19
z	Number of tooth	$z = D/m$	40	20
α	Clutch angle, degree	-	20	20
α_f	Face clutch angle, degree	$\tan\alpha_f = \tan\alpha/\cos\beta$	43.2	43.2
β	Helix angle, degree	-	20	20
D	Pitch diameter, mm	$D = m_n z / \cos\beta$	127.7	63.85
D_o	Outside diameter, mm	$D_o = D+2a$	133.7	69.85
D_R	Root diameter, mm	$D_R = D-2b$	120.2	60.1
p_n	Normal pitch, mm	$p_n = m_n \pi$	9.42	9.42
p_f	Face pitch, mm	$p_f = m_f \pi$	10.05	10.05
h	Height of tooth, mm	$h = a+b = 2.25m$	6.75	6.75
b	Dedendum, mm	$b = 1.25m$	3.75	3.75
t	Thickness of tooth, mm	$t = p/2$	4.71	4.71
s	Space of tooth, mm	$s = p/2$	4.71	4.71
b	Face width, mm	-	2	2

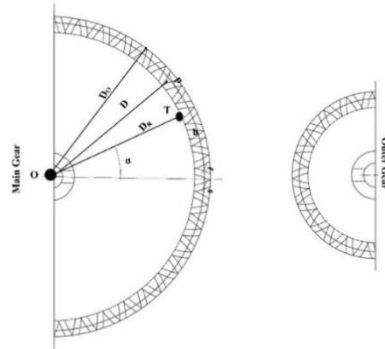


Figure 3.7 Technical Drawing of the Gears

3.2. Design of Robot Structure

In structural design of the robot, connection of transmission system and chassis were considered to be rigid and durable for both ladder-climbing and straight road motions. In designing process, structural parts of the robot were categorized as industrial products and parts that will be produced.

Modular chassis of the system were considered to have suitable positions for actuator of the system and linear actuation mechanism. Designed modular chassis provides opportunity to remove required profiles for easy-to-assemble and makes design easily changeable. General design for system with transmission system was shown in Figure 3.8.

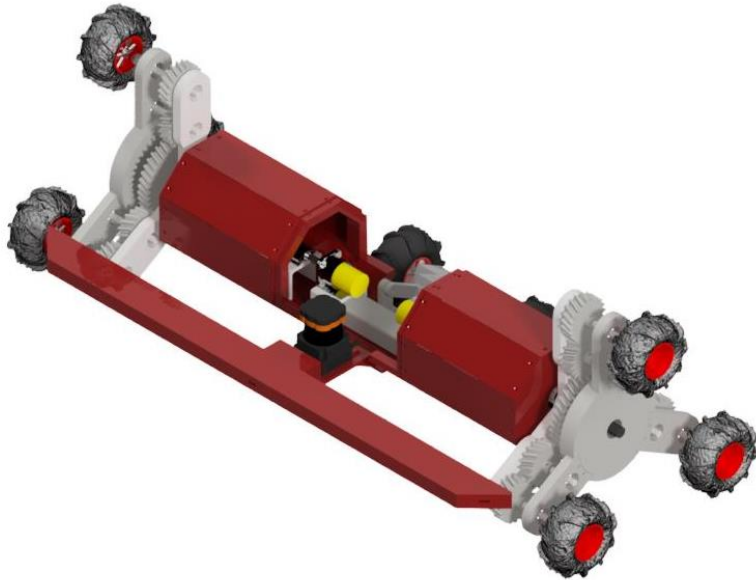


Figure 3.8 General System Design

System weight and dimensions has crucial importance for all mobile robots for maneuverability, energy consumption and performance at completing the tasks. In designing process, these parameters were considered to design chassis with minimal dimensions for bot electrical and mechanical system to succeed in its task.

Dimensions of structure of ladder climbing robot are given in Figure 3.9. Designed system has 792 mm length. Distance between two sides of gear-sets is 464 mm with chassis length of 382 mm. Distance between inner side of inner cover to outer side of outer cover is about 70 mm. Ladder climbing robot has 346 mm height, 466 mm width. Rotation radius of the system is 210 mm with chassis radius of 150 mm.

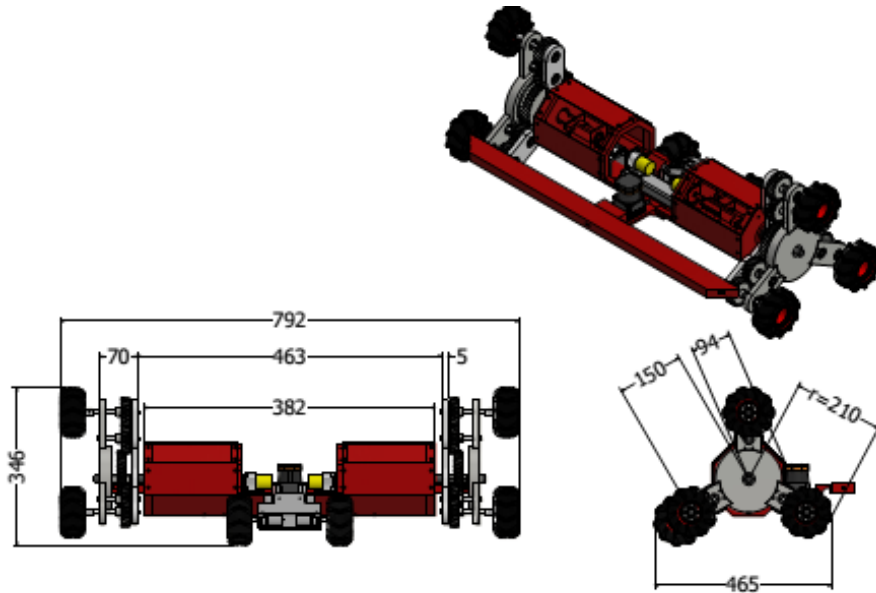


Figure 3.9 Dimensions of Ladder Climbing Robot in mm

3.2.1. Design of Linear Actuation Mechanism

Linear actuation mechanism were designed to satisfy system needs such as linear velocity, acceleration and torque. Industrial linear motors does not meet the stroke and torque requirement in our system to push or pull main gear. Designed linear actuation mechanism with explanation is given in Figure 3.10 and Table 3.2.

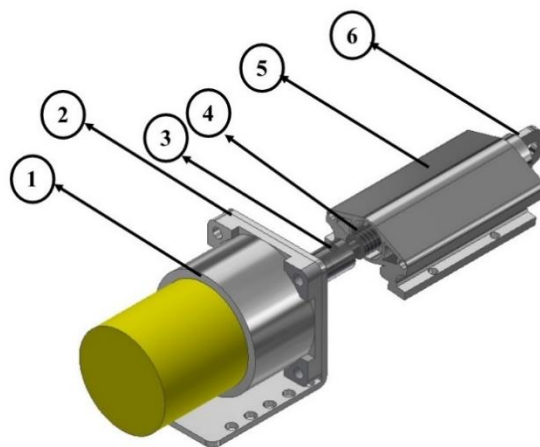


Figure 3.10 Designed Linear Actuation Mechanism

Table 3.2 Explanation of Linear Actuation Mechanism Components

No	Name of the Component	Explanation
1	DC Motor	It is primary element of designed system with metal geared reduction system. Selected motor has 32 Watt power and 450 N load capacity.
2	Bracket	It was used to connect DC motor to chassis.
3	Steel Coupling	It was used to connect DC motor shaft to threaded shaft.
4	Threaded Shaft	M10x1.5 threaded shaft was used to transform rotational motion to linear motion.
5	Cover	Linear actuator cover was used to connect system to chassis.
6	Connection Shaft	Connection shaft was used to transfer linear motion.

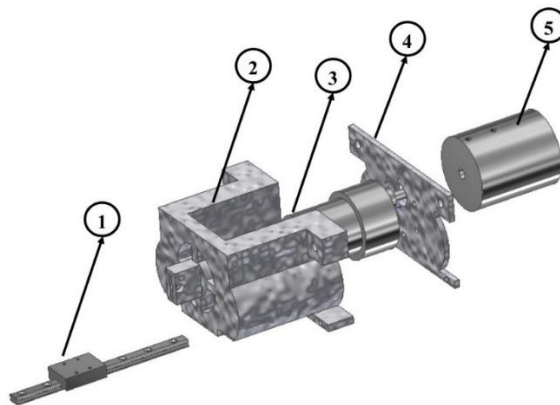


Figure 3.11 Designed Motion System

Designed motion system for ladder climbing robot consists of five different components as shown in Figure 3.11. In motion design, linear rail and car (1) was used to support DC motor cover (2) with DC motor cover case (4) that is used to connect motor during transitional motion through transformation system and protection of motor, from ladder climbing mode to straight road mod or vice versa.

In this system, DC motor (3) was selected to actuate gearset. Connection coupling (5) was used to connect shaft of DC motor to gearset.

Final and assembled designs for transmission system are given in Table 3.3 and Figure 3.12 with explanation of used components.

Table 3.3 Components of Transmission System with Explanation

No	Name of the Component	Explanation
1	Linear motion ball Bearing	It was selected to provide both axial and radial motions to transmission system.
2	Bearing segment	It was used to fix the ball bearing and to make the motion and transmission system coaxial.
3	Inner housing covers	Transmission system elements were supported with outside-inside housing covers.
4	Main gear	The required torque and angular velocity were distributed by the main gears for linear and rolling motions.
5	Inner-outer gears	They were used to transmit the motion from main gear to wheels.
6	Ball bearings	They were used for housing of inner-outer gear shafts.
7	Shaft segment	It was used to fix the shafts and to avoid from axial misalignment.
8	Outer housing cover	Transmission system elements were supported with outside-inside housing covers.
9	Shaft to wheel connector	The connection of the wheels and shafts were provided with these components.
10	Off-road wheel	They were used for traction of the system.

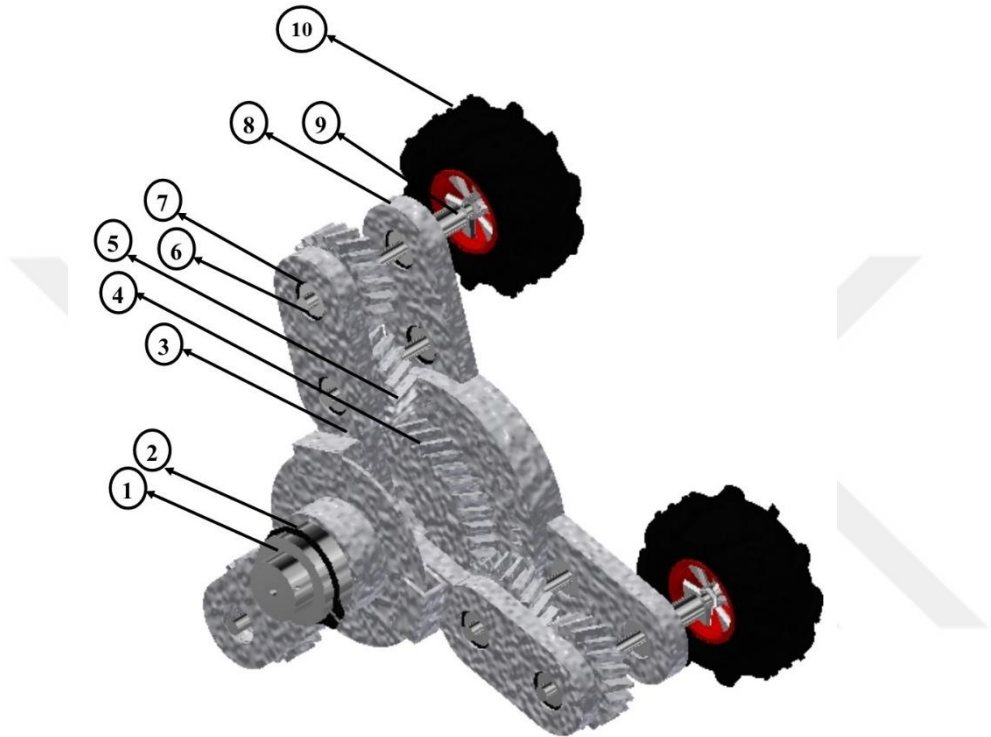


Figure 3.12 Designed Transmission System

3.3. Verification of Designed System

Designed system was subjected to numerical and analytical calculations and analysis to obtain occurred forces and torques during ladder climbing and straight road motion. Calculated torque, power and velocity values were used for defining requirement of DC Motor and power supply.

In verification step of design, four different materials were applied to the system during analysis. Weight of the robot was calculated for each material and safety factor for critical components were calculated. Applied materials are; PLA, ABS, Aluminum 6061 and S 235 and properties are given in Table 3.4.

Table 3.4 Mechanical Properties of Materials

	PLA	ABS	Al 6061	S 235
Density (g/cc)	1.25	1.21	2.70	7.80
Yield Strength (MPa)	59	51.7	55.2	205
Ultimate Tensile Strength (MPa)	73	55	124	415
Young's Modulus (GPa)	1.28	1.1	68.9	205

In numerical calculations, PLA defined robot were analyzed to calculate torque and velocity values. Then, analytical calculations were applied for same components to cross-check correctness of numerical and analytical solutions.

3.3.1. Analytical Calculations for Ladder Climbing Robot

3.3.1.1. Motion Calculation

Motion calculation of ladder climbing robot were conducted to calculate forces that acted on components and actuation calculations.

For analytical calculations, ladder climbing robot's free body diagram was modelled as rolling down object on an inclined plane. This calculation approach was used to accomplish analytical calculations. Angle of slope on rolling down object was also calculated using ladder dimensions (Figure 3.13).

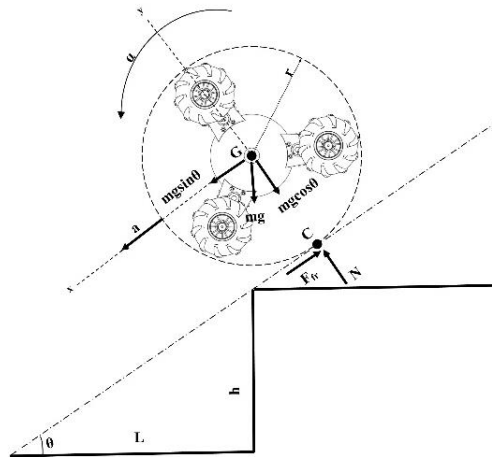


Figure 3.13 Rolling Down on an Inclined Plane Assumption

Dimensions of ladder for step of a ladder for h (height) and L (length) parameters were defined as 150 and 300 mm, respectively. These parameters define the angle of slope of ladder as 30° . Using this free body diagram, the forces, acceleration, torque requirement, and power were calculated.

Calculation assumption for equilibrium proves that if the reverse parameters that were calculated analytically are applied to the system as reverse, that will create a balance that blocks rolling motion, which is the required minimum parameters for rolling up motion.

Acting Forces on System

$$\Sigma F_x = mg \sin \theta - F_{fr} = ma \quad (3.1)$$

$$N - mg \cos \theta = 0 \quad (3.2)$$

Acting Moments on System

$$\Sigma M_g = I\alpha \quad (3.3)$$

$$Fr = mr^2\alpha \quad (3.4)$$

In the calculations, if the maximum force derived from the mass and the maximum translational acceleration of the robotic system was larger than the slippage force

caused from the relation of wheel and ground, the rolling motion occurred as desired.

$$F_{\max} = ma_m \quad (3.5)$$

$$mg \sin 30^\circ - F_{fr} = ma \quad (3.6)$$

$$T = I\alpha \quad (3.7)$$

$$F_{fr}r = \frac{1}{2}mr^2 \frac{a}{r} \quad (3.8)$$

$$F_{fr} = \frac{1}{2}ma \quad (3.9)$$

$$mg \sin 30^\circ - \frac{1}{2}ma = ma \quad (3.10)$$

$$mg \sin \theta = \frac{3}{2}ma = F_{\max} \quad (3.11)$$

The maximum force was equal to $3/2ma$ as found in Equation 3.11.

$$T = I\alpha \quad (3.12)$$

$$F_{fr}r = \frac{1}{2}mr^2 \frac{a_m}{r} \quad (3.13)$$

$$F_{fr} = \frac{1}{2}ma_m \quad (3.14)$$

$$a_m = \frac{2F_{fr}}{m} = \frac{2mg \cos \theta \mu}{m} \quad (3.15)$$

$$a_m = 2g \cos \theta \mu \quad (3.16)$$

The maximum translational acceleration was found using the torque equations.

In the rolling torque calculations:

$$T = I\alpha \quad (3.17)$$

$$F_{fr}r = \frac{1}{2}mr^2 \frac{a}{r} \quad (3.18)$$

$$F_{fr} = \frac{1}{2}ma \quad (3.19)$$

$$mg \cos \theta \mu = \frac{1}{2}ma \quad (3.20)$$

$$g \cos \theta \mu = \frac{1}{2}a \quad (3.21)$$

$$\mu = \frac{a}{2g \cos \theta} \quad (3.22)$$

$$F = ma \quad (3.23)$$

$$mg \sin \theta - mg \cos \theta \mu = ma \quad (3.24)$$

$$g \sin \theta - g \cos \theta \mu = a \quad (3.25)$$

$$g \sin \theta - g \cos \theta \frac{a}{2g \cos \theta} = a \quad (3.26)$$

$$g \sin \theta = \frac{3}{2}a \quad (3.27)$$

$$a = 2/3g \sin \theta \quad (3.28)$$

Then total rolling torque was the sum of the rotational and the translational moments:

$$\Sigma M = \frac{1}{2}mr^2 \frac{a}{r} + mar \quad (3.29)$$

$$\Sigma M = \frac{1}{2} mar + mar \quad (3.30)$$

$$\Sigma M = 3/2mar \quad (3.31)$$

The rolling torque was equal to $3/2mar$ as found in Equation 3.31.

Where:

ΣF_x	Total translational force
N	Reaction force at the point of C
$I\alpha$	Torque
F_{fr}	Friction force
a	Translational acceleration
a_m	Maximum translational acceleration
α	Angular acceleration
F_s	Slippage force
μ	Static friction coefficient

Calculation of the maximum force, acceleration for rolling motion without slippage and rolling torque were conducted using MATLAB Software as shown in Figure 3.14.

Calculation parameters used in equations:

m (total mass for PLA)	10.5 kg
μ (Static friction coefficient)	0.75
g (Standard earth gravity)	9.81 m/s ²
r (Radius of the robotic system)	210 mm

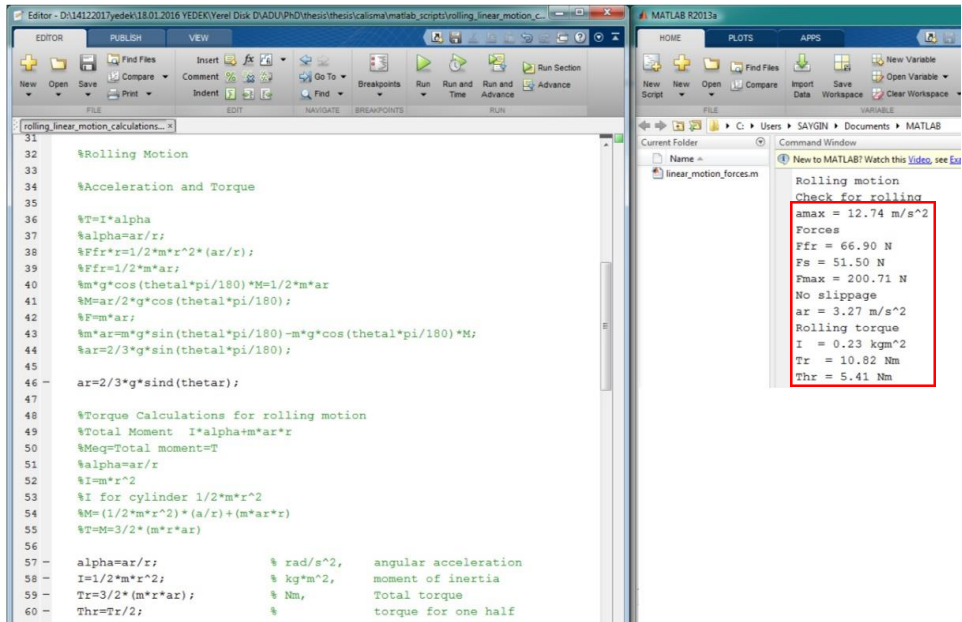


Figure 3.14 Torque and Acceleration Calculations for Rolling Motion

Slippage check was accomplished by making comparison between maximum force and slippage. These calculations shows that maximum force that equals to 200.7 N was larger than slippage force that equals to 51.5 N that provides rolling motion as desired.

Angular velocity and power of the system can be calculated using these formulas;

$$w = \frac{d\theta}{dt} = \dot{\theta} \quad (3.32)$$

$$\alpha = \frac{d\omega}{dt} = \dot{\omega} = \ddot{\theta} \quad (3.33)$$

$$V = \dot{r} = \omega r \quad (3.34)$$

$$P = T\omega \quad (3.35)$$

In climbing motion, designed system was set as 1m/s linear velocity and angular velocity was calculated based on linear velocity. Then, angular velocity and power calculations for rolling motion were accomplished using Matlab.

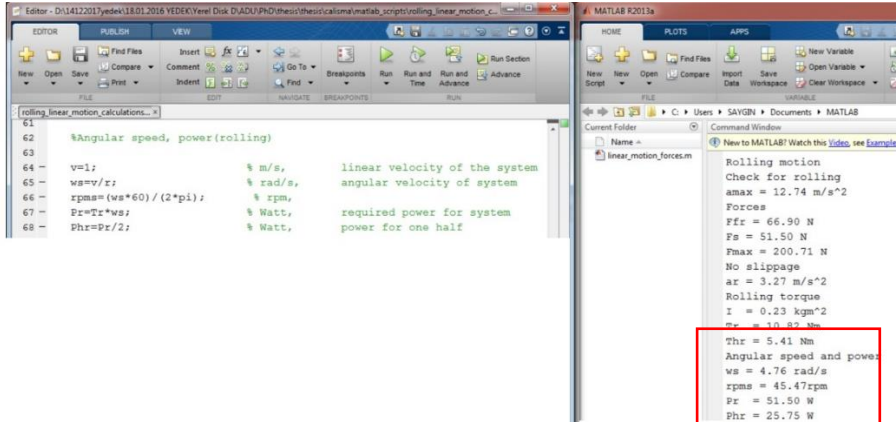


Figure 3.15 Angular Velocity and Power Calculations for Rolling Motion

In linear motion, angle of slope and linear speed was specified as 20° and 1 m/s , respectively. Reaction forces and resistance forces such as gradient, acceleration and rolling, and torque & power and angular velocity requirement were calculated (Figure 3.16).

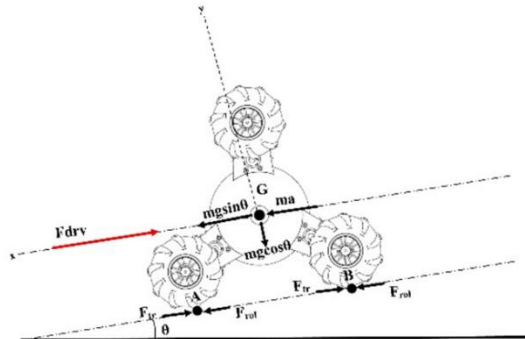


Figure 3.16 Effected Forces of Body

$$\Sigma F_x = 0 \quad (3.36)$$

$$mg \sin \theta - F_{rol} - ma + F_{drv} = 0 \quad (3.37)$$

$$F_{rol} = mg \cos \theta c_{rol} \quad (3.38)$$

$$F_{drv} = mg \sin \theta + F_{rol} + ma \quad (3.39)$$

$$T = mg(\sin \theta + F_{fr})r \quad (3.40)$$

$$P = \frac{F_{drv} v}{e} \quad (3.41)$$

$$w_o = v / r_o \quad (3.42)$$

$$w_m = w_o r_o / r_m \quad (3.43)$$

For verification stage, rolling coefficient was selected as 0.02 and efficiency of gear system was used as 0.8 for analytical calculations. Radius of outer gear and main gear were 30 and 60 mm, respectively. Calculation of angular speed, torque and power requirement for linear motion is given in Figure 3.17

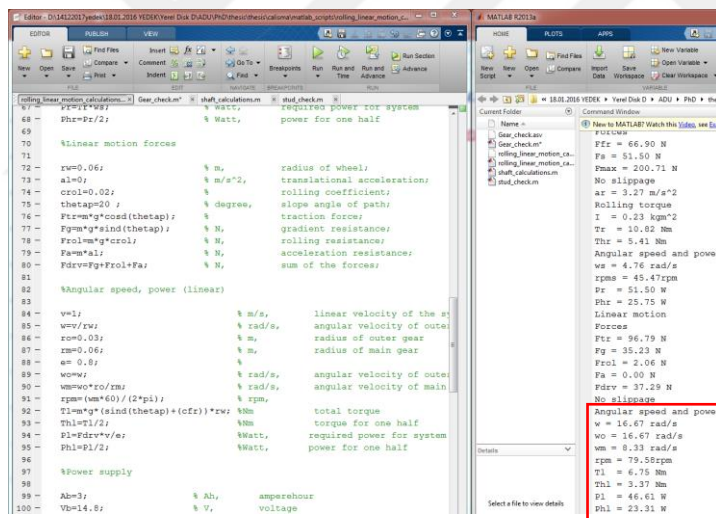


Figure 3.17 Angular Velocity, Torque and Power Calculations for Linear Motion

3.3.1.2. Mechanical Strength Check of Critical Components

Strength validation of the components were applied to calculate & validate proper gear modules and minimum shaft and coupling diameter.

Minimum shaft diameter for main, inner & outer shaft were calculated under dynamic loads with consideration of velocity & torque values that were calculated in motion calculation. These calculation were conducted with the tangential, normal and radial forces occurred on gears (Figure 3.18)

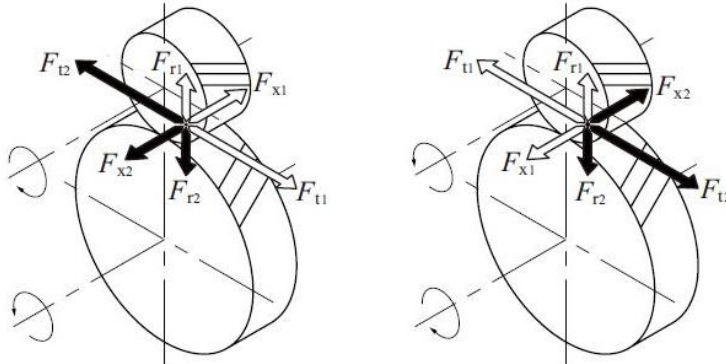


Figure 3.18 Occurred Forces on the Gears

$$Ft_1 = Ft_2 = \frac{2Mr_1}{d_1} \quad (3.44)$$

$$Fn_1 = \frac{Ft_1}{\cos \alpha} \quad (3.45)$$

$$Fr_1 = Fr_2 = Ft_1 \tan \alpha \quad (3.46)$$

For shaft of main gear, reaction forces for each joints as A & B and bending moment at center of the main gear were calculated for x-y and x-z planes. Technical drawing of the main shaft with shear-and-moment diagram is shown in Figure 3.19.

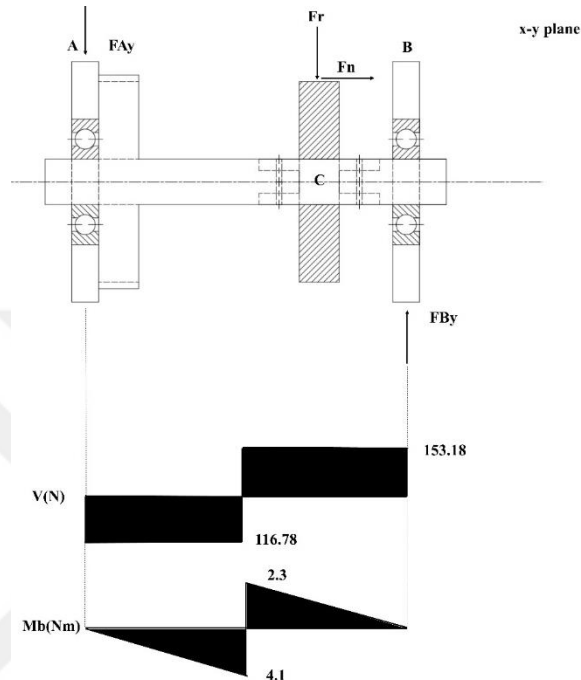


Figure 3.19 Technical Drawing of the Main Shaft with Shear-and-Moment Diagram

Minimum shaft diameters were calculated using equations 3.47 and 3.48 (Sekercoglu, 2015).

$$d = \sqrt[3]{\frac{32 \times S}{\pi} \sqrt{\left(\frac{Me}{\sigma * TDE}\right)^2 + \frac{3}{4} \left(\frac{Md}{Re}\right)^2}} \quad (3.47)$$

$$\sigma *_{TDE} = \frac{(Ky)(Kb)(\sigma TDE)}{Kc} \quad (3.48)$$

Where;

S	Factor of safety	3
σ_{TDE}	Full variable stress strength of material	180 MPa
Re	Yield strength	235 MPa

K_b	Shape coefficient	0.95
K_y	Surface coefficient	0.9
K_c	Notch effect	1.2

Material of shafts were selected as S 235 steel for each material configuration. After calculation for minimum shaft diameters, 6 and 2 mm thicknesses were added to diameter to equalize effect of shoulder and depth of the connection pin (Figure 3.20).

```

55
56 - FRr=(FAy^2+FRz^2)^(1/2);
57 - FRz=(FBz^2+FRy^2)^(1/2);
58
59 %Resultant bending moment
60
61 - MBr=(MBc1^2+MBc3^2)^(1/2); %Nm
62
63 %Shaft diameter
64
65 - qTDE=180; %N/mm^2 for S235 steel, Fully variable strength of mater:
66 - Re= 235; %N/mm^2 yield strength
67 - Kb=0.95; %shape coefficient
68 - Ky=0.9; %surface coefficient
69 - Kc=1.2; %notch effect
70 - S=3; %safety factor
71 - t1=6; %depth of key or pin
72 - d=(MBr*1000)/(qTDE*Kb*Ky/Kc*S); %minimum diameter loads

```

The screenshot also shows the MATLAB Command Window with the following output:

```

Main Shaft
Ftm = 100.00 N
Frm = 106.42 N
Frm = 36.40 N
FBy = 153.18 N
FAy = 116.78 N
MBc1 = 4.09 Nm
MBc2 = 2.30 Nm
FBz = 70.00 N
FAz = 30.00 N
MBc3 = 1.05 Nm
FRz = 120.57 N
FRr = 168.42 N
MBr = 4.22 Nm
d = 16.52 mm

```

Figure 3.20 The Minimum Shaft Diameter Calculation of Main Shaft

Gear selection and verification of gears were calculated according to the broken at tooth bottom and surface pressure. Module verification with calculations were applied to outer gear as that has less strength and exposed to more rpm and load cycle.

Module verification according to the broken at tooth bottom (Sekercioglu, 2015):

$$\sigma_{sf} = \frac{(K_b)(K_y)\sigma_{TD}}{(K_c)(S)} \quad (3.49)$$

$$\sigma_{TD} \cong 0.7\sigma_{FE} \quad (3.50)$$

$$m \geq \sqrt[3]{\frac{2(Mr)(Kf)(Ki)(Kv)(K\varepsilon)(Km)}{(\psi m)(z)(\sigma_{sf})}} \cos \beta \quad (3.51)$$

Where:

σ_{sf}	Allowable stress	4.375 MPa
S	Factor of safety	3
σ_{TD}	Full variable stress strength of material	21 MPa
FE	Continuous strength	30 MPa
Kb	Shape coefficient	1
Ky	Surface coefficient	0.75
Kc	Notch effect	1.2
Mr	Moment	3 Nm
Kf	Form coefficient	2.4
Ki	Operation coefficient	1.25
Kv	Speed coefficient	1
K ε	Clutch ratio coefficient	1
Km	Load distribution coefficient	1.2
ψm	Module width coefficient	15
z	Number of teeth	20

The continuous strength of the gears material was assumed equal to yield as they were manufactured with PLA which was brittle.

The module check according to surface pressure (Sekercioglu, 2015):

$$P_{sf} = \frac{(\sigma_H)(Kp)}{S} \quad (3.51)$$

$$m \geq 0.7 \cos \beta \sqrt[3]{\frac{2(Mr)(Ki)(Kv)(Km)(K\varepsilon)E(P_{12} + 1)}{(\psi_m)(z^2)(P_{sf}^2)(P_{12})}} \quad (3.52)$$

Where:

P_{sf}	Allowable pressure	10 MPa
σ_H	Continuous surface pressure strength	30 MPa
S	Factor of safety	3
Mr	Moment	3 Nm
Ki	Operation coefficient	1.25
Kv	Speed coefficient	1
$K\varepsilon$	Clutch ratio coefficient	1
Km	Load distribution coefficient	1.2
ψ_m	Module width coefficient	15
z	Number of teeth	20
E	Elastic Modulus	1,100 MPa

P12 Gear ratio 2

The mechanical safety of the studs used as pin on the coupling for DC motor, main shaft connection was checked according to torsion stress.

$$\sigma_{sf} = \frac{Mr}{Wt} = \frac{16(Ft)r}{(\pi)(dp^3)} \leq \frac{Re}{S} \quad (3.53)$$

$$Ft = \frac{2Mr}{(z)(Do)} \quad (3.54)$$

Where:

σ_{sf}	Allowable stress	116.67 MPa
S	Factor of safety	3
Mr	Moment	6 Nm
Wt	Torsion strength moment	290.42 mm ³
Ft	Tangential force	352.94 N
Re	Yield strength	350 MPa
z	Number of pin	2
Do	Inner diameter of coupling	17 mm
dp	Pin diameter	5 mm

Calculations for the coupling pin check were also calculated with MATLAB Software (Figure 3.21).

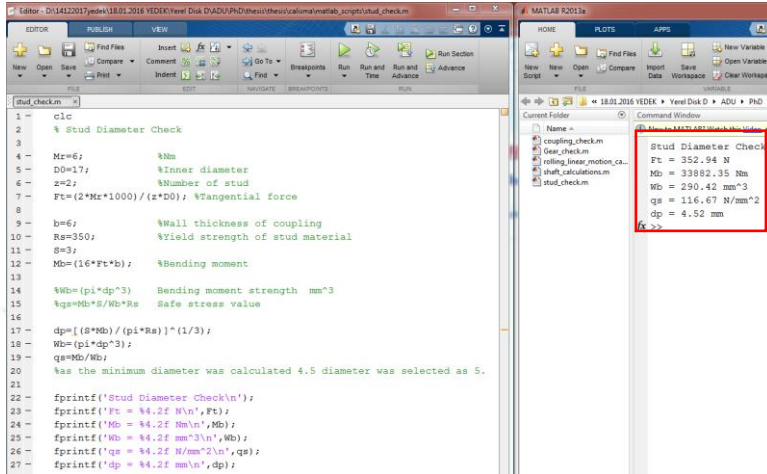


Figure 3.21 Coupling Pin Diameter Calculation

Calculations that were mentioned above were used to develop a motion and strength calculator to conduct required calculations using Visual Studio interface with C# programming language (Figure 3.22).

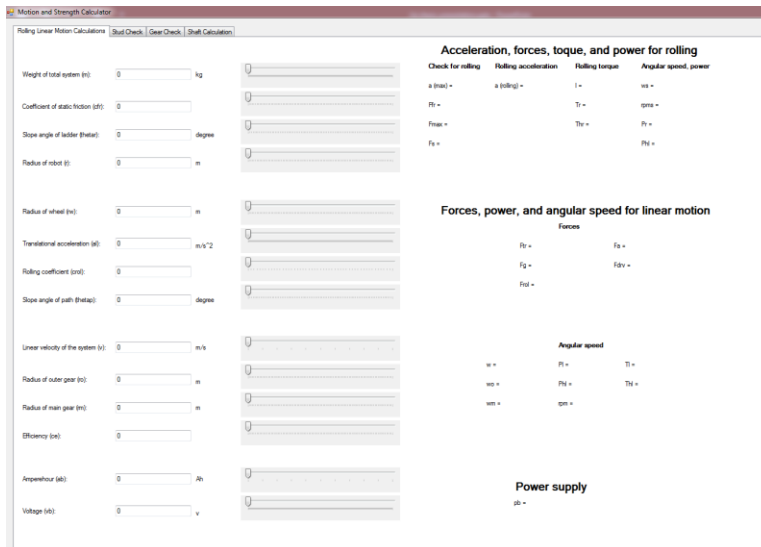


Figure 3.22 Motion and Strength Calculator

3.3.2. Numerical Analysis for Ladder Climbing Robot

Numerical analysis were accomplished in two stage for four different materials. Analysis were carried out using ANSYS Rigid Body Dynamics and Static Structural module.

Each scenarios were modelled for motion and strength check calculation.

3.3.2.1. Motion Analyses

Motion analyses of Ladder Climbing robot for both ladder climbing and straight road motion were modelled and applied. In ladder climbing motion, half of the robot were modelled to reduce simulation time using advantage of symmetrical design.

For ladder climbing motion, four boundary conditions were defined as back motor and right motor, earth gravity and remote force (Figure 3.23)

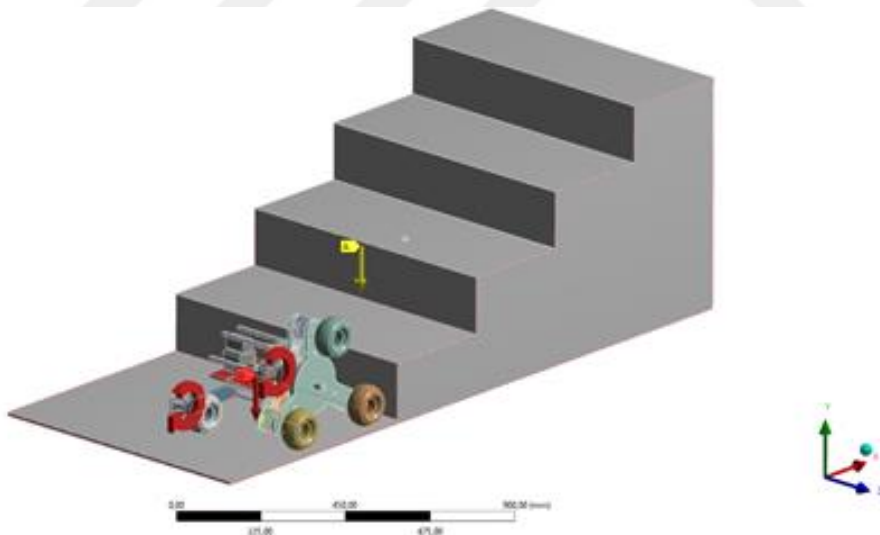


Figure 3.23 Modeling of Ladder Climbing Motion

For this simulation, half of the body was suppressed by utilizing from symmetry of the body to decrease simulation time. Suppression of half of the body was decreased the weight of the system. To eliminate this disadvantage half of the system load was applied to the robot as remote force.

In rigid body analysis for ladder climbing motion, six different output parameters were set (Figure 3.24).

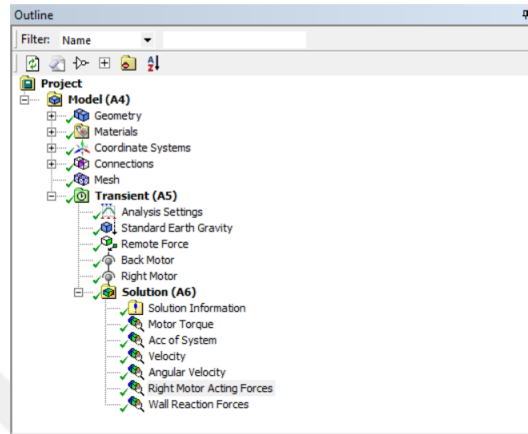


Figure 3.24 Output Parameters of Ladder Climbing Motion Analysis

In straight road motion, four boundary conditions were defined as back motor, right, and left motor and earth gravity (Figure 3.25).

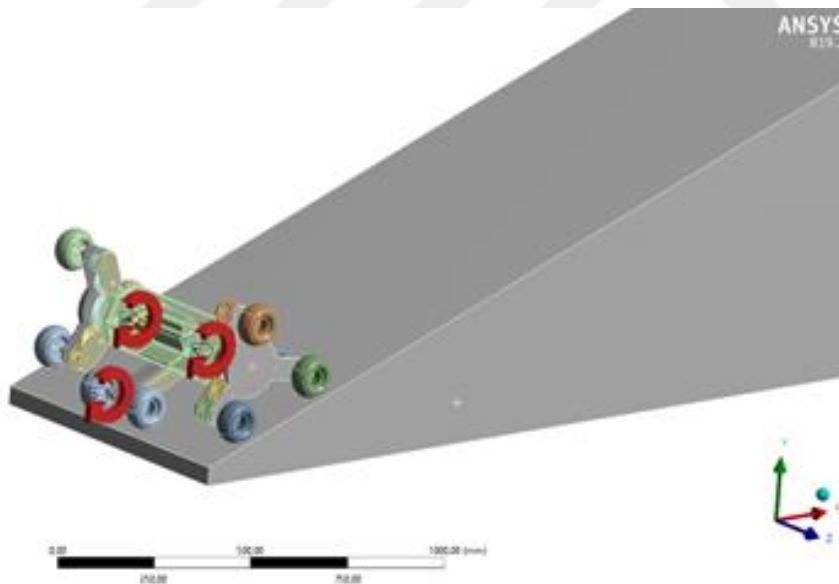


Figure 3.25 Modeling of Straight Road Motion

Transmission relationships between gears in this simulation were applied using constraint equations. In this simulation, actuation of the system for left and right transmission system was actuated from Joint Rotation from motor in each side. Constraint equations were defined for each gear relationship to provide ratio between gears and main gears (Figure 3.26).

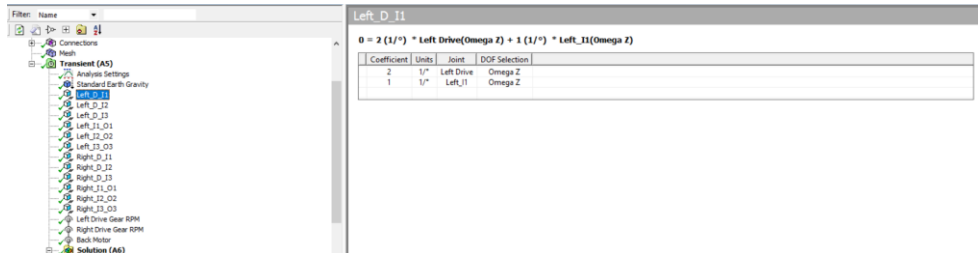


Figure 3.26 Constraint Equation for Gear Transmission

In rigid body analysis for straight road motion, six different output parameters were set (Figure 3.27).

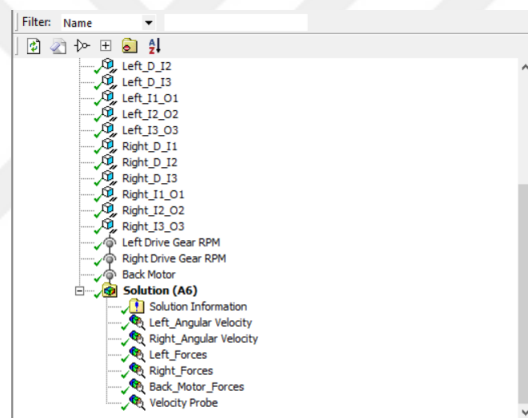


Figure 3.27 Output Parameters of Straight Road Motion Analysis

3.3.2.2. Mechanical Strength Check of Critical Components

In numerical analysis for material strength check, three components were specified as critical components and analyzed. These components are:

- Inner Gear
- Inner & Outer Shaft
- Main Shaft

Inner gear was selected as critical component for both analytical and numerical strength check calculations because of its less strength and being exposed to more rpm and load cycle. In the analysis, torque that is acquired from rigid body dynamics were applied to the gear (Figure 3.28 Boundary Conditions of Outer Gear Figure 3.28).

A: Static Structural
 Static Structural
 Time: 1, s
 12.01.2020 12:38

- A** Standard Earth Gravity: 9806,6 mm/s²
- B** Fixed Support
- C** Joint - Moment

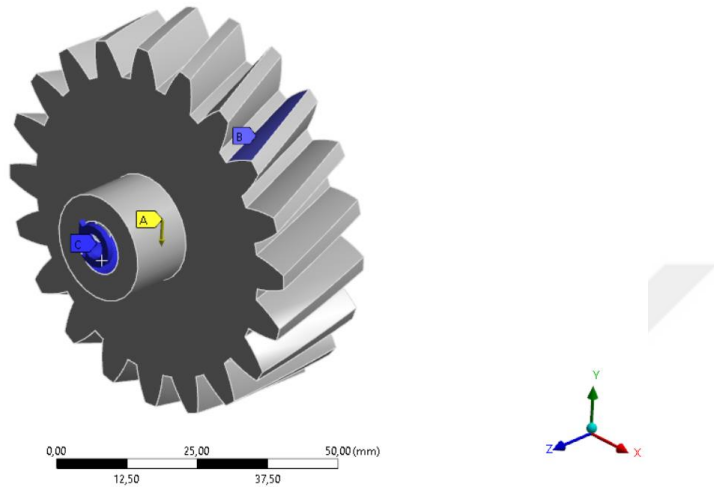


Figure 3.28 Boundary Conditions of Outer Gear

Inner and outer shafts are selected are critical. These shafts and loads on gears are equal because of gear modules and number of teeth and only one shaft is analyzed.

Main shaft is mounted to roller bearings and fixed to main gear. Maximum torque was applied to main shaft and using conditions that acquired from rigid body dynamics analyzes simulation of main shaft was accomplished. For main shaft analysis, three boundary conditions were applied as fixed support, moment that is acquired from rigid body dynamics analysis and gravity (Figure 3.29).

A: Static Structural
 Static Structural
 Time: 1, s
 12.01.2020 12:23

- A** Standard Earth Gravity: 9806,6 mm/s²
- B** Fixed Support
- C** Moment

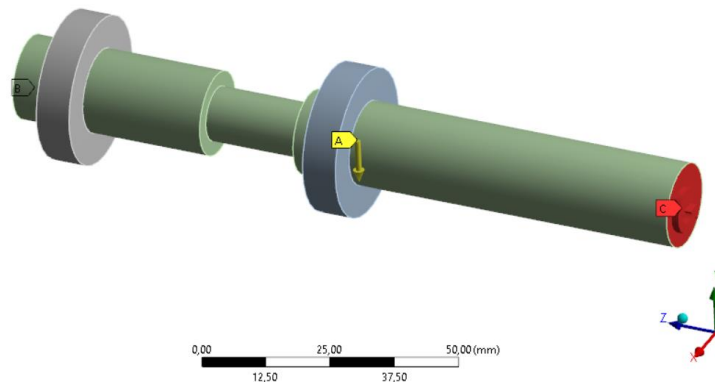


Figure 3.29 Boundary Conditions of Main Shaft

4. RESULTS AND DISCUSSION

In this chapter of the thesis, analytical and numerical analyses results were presented and explained.

4.1. Verification of Motion Modelling and Analytical Calculation

Designed ladder climbing robot mechanism was analyzed in ANSYS Rigid Body Dynamics model for PLA material that is accepted as prototyping material. Several components such as shafts, couplings and wheels' materials were defined for their specific materials as S 235 and rubber. Other components of the system were tested for four different materials as S 235, Al 6061, ABS and PLA. Designed systems and their weights were given in Table 4.1.

Table 4.1 Weight of System for Different Material Configuration

	ABS	PLA	ST	AL
Weight (kg)	9.542	10.592	44.154	18.322

Analytical and numerical calculation could have differences because of the calculation method. Numerical analyses has some error ratio because of their solving technique but for complicated systems, these solutions are acceptable.

Designed and modelled ladder climbing robot were both calculated for PLA defined calculation sets to make comparison about their results to ensure that modelled system has high correctness.

In analytical calculation, an assumption was made to apply an equilibrium to calculate minimum torque requirement to block rolling motion of system to downward that mean larger torques will create rolling motion to upwards. For calculations, system configuration with PLA material was selected and equations 3.1 to 3.43 were applied. Calculations of the system showed that designed system for 1 m/s linear motion has 3.27 m/s² rolling acceleration and requires 10.8 Nm torque for total system. Also, rotational velocity of rolling motion was calculated as 46 rpm and power requirement of the system is 52 Watt.

Same parameters that were obtained from analytical calculations were modelled in Rigid Body Dynamics analyses to compare and check the results for both ladder climbing and straight road motion.

For ladder climbing motion, analysis for motor torque on z-axis showed that motor requirement of system has 5.062 Nm torque requirement for each motor, which is almost half of the system that calculated in analytical calculations. Acceleration of the system is also almost equal to the analytical calculations.

Details of "Acc of System"	
Definition	
Type	Acceleration
Location Method	Geometry Selection
Geometry	1 Body
Orientation	Global Coordinate System
Suppressed	No
Options	
Result Selection	All
<input type="checkbox"/> Display Time	End Time
Results	
<input type="checkbox"/> X Axis	1093,6 mm/s ²
<input type="checkbox"/> Y Axis	-3348,2 mm/s ²
<input type="checkbox"/> Z Axis	4,7121e-012 mm/s ²
<input type="checkbox"/> Total	3522,3 mm/s ²
Maximum Value Over Time	
Minimum Value Over Time	

Figure 4.1 Acceleration Results of System in Numerical Analysis

Results that obtained from comparison of analytical calculations and numerical analyses showed that modelling of the system and solution approach for analytical calculation has almost same values for both torque and acceleration of the system.

Using these values, model of the system can be accepted as correct and obtained results for other materials can be significant.

4.2. Numerical Analyses for Motion Calculations

Motion calculations for ladder climbing motion and straight road motion were calculated using numerical analysis. In analysis, two different analyses set were

modelled for straight road and ladder climbing mode and each analyses' set were solved for four different material set.

Table 4.2 Power Requirement and Torque Values For Each Configuration

	ABS	PLA	ST	AL
Weight (kg)	9.542	10.592	44.154	18.322
Torque for Ladder Climbing Motion (Nm/Motor)	4.614	5.062	12.967	8.464
Torque for Straight Road Motion (Nm/Motor)	3.425	4.652	10.781	7.325
Power Requirement for Ladder Climbing Motion (Watt)	44.45	48.77	124.94	81.55
Power Requirement for Straight Road Motion (Watt)	32.99	44.82	103.88	70.58

Analyses results for ladder climbing and straight road motion for each material were given in Table 4.2.

In structural analysis, output data of analyses will be used to calculated mechanical strength of the material. Selected critical components inner & outer shafts and main shaft will be analyzed using larger torque values with S 235 material because of using same material for all configurations. Inner gear analyzes will be accomplished using different materials using larger torque values for each material configuration.

4.3. Numerical Analyses for Mechanical Strength

Mechanical strength value for critical components were studied using finite element methods to determine selected material for specified load conditions are safe or not.

In analyses for inner shaft, torque values that occurred due to material loads were divided by two to mechanical transmission and applied to shaft and gears. Determined loads and mechanical output of the analyses is given in Table 4.3 for S235 material.

Table 4.3 Safety Factor and Occurred Stresses on Inner Shaft

	ABS	PLA	ST	AL
Applied Torque (Nm)	2.307	2.526	6.483	4.232
Equivalent Max Stress (MPa)	36.993	40.505	103.96	67.861
Maximum Shear Stress (MPa)	21.352	23.379	60.002	39.169
Safety Factor for Equivalent Max Stress	3.466	3.1663	1.2337	1.8899
Safety Factor for Maximum Shear Stress	3.003	2.7428	1.0687	1.6372

Designed shaft for inner and outer gear was suitable to use in robot structure that manufactured using PLA or ABS material that is used in additive manufacturing techniques. Safety factor shows that steel and aluminum chassis will not work without failure of inner and outer shafts.

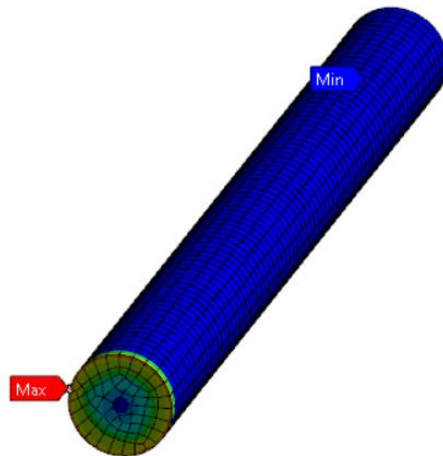


Figure 4.2 Results of the Structural Analysis of Inner Shaft

In analyses for main shaft, torque values that occurred due to material loads were applied to shaft. Determined loads and mechanical output of the analyses is given in Figure 4.3 for S235 material.

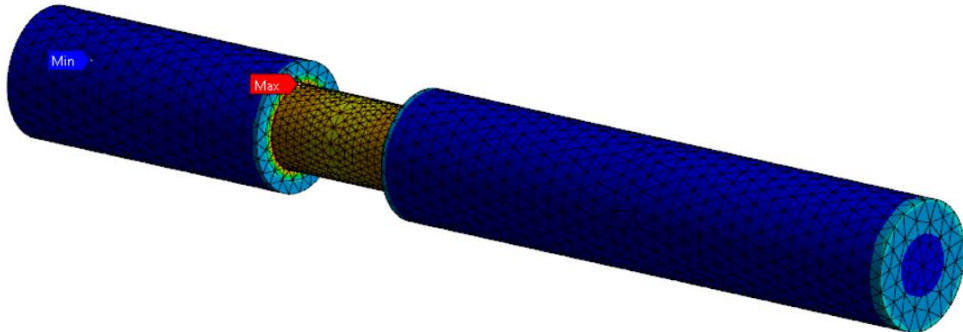


Figure 4.3 Results of the Structural Analysis of Main Shaft

Table 4.4 Safety Factor and Occurred Stresses on Main Shaft

	ABS	PLA	ST	AL
Applied Torque (Nm)	2.307	2.526	6.483	4.232
Equivalent Max Stress (MPa)	16.497	18.06	46.321	30.243
Maximum Shear Stress (MPa)	9.5228	10.426	26.743	17.464
Safety Factor for Equivalent Max Stress	7.7743	7.10	2.7687	4.2407
Safety Factor for Maximum Shear Stress	6.7338	6.15	2.3978	3.6727

Using structural analysis, inner gear that is used in transmission for straight road motion were analyzed. In each material configuration, gear material was selected as the same material that was used in robot structure.

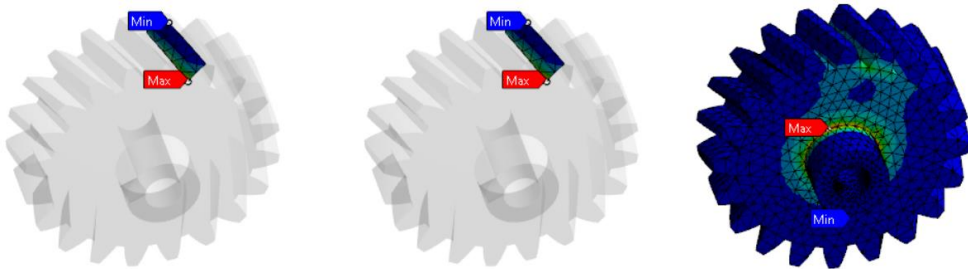


Figure 4.4 Results of the Structural Analysis of Gear

In this analysis, inner gear was subjected to half of the motor torque that obtained from straight road motion analyzes because of transmission of power. Results that obtained from analyzes are given in Table 4.5.

Table 4.5 Stress and Safety Factor for Inner Gear

	ABS	PLA	ST	AL
Applied Torque (Nm)	1.712	2.326	5.390	3.662
Surface Equivalent Stress (MPa)	0.87	1.18	2.81	1.88
Surface Shear Stress (MPa)	0.50	0.68	1.62	1.08
Max Equivalent Safety Factor	3.44	2.54	15	15
Max Shear Safety Factor	2.98	2.19	15	15

According to selected module, connection grove and number of teeth of gear; aluminum and steel materials has more strength than required. PLA or ABS based chassis will be the most suitable option for inner gear from PLA material.

5. CONCLUSIONS

In this thesis, study of mechanism that can climb over an object and ladders was designed with linear actuation mechanism. Designed system was modelled using both commercial components and components that will be manufactured.

Ladder climbing robot design was modeled using two scenarios as ladder climbing mode and straight road mode. Numerical analyzes and analytical calculations were applied to these models to ensure about correctness about numerical analysis model and to obtain occurred loads on robot structure. Robot structure was modeled using four different materials as PLA, ABS, Aluminum 6061 and S 235.

In ladder climbing robot design, three components were specified as critical and analyzes were applied to them. According to criteria of power consumption, PLA and ABS materials gave best solution for manufacturing designed system and apply for industrial or domestic applications. According to mechanical strength, PLA based chassis for inner shaft strength and gear manufactured with PLA were specified as optimum material. For comparison of the strength of main shaft for each material configuration of chassis, PLA and ABS based materials defines that designed shaft material is required to change or diameter of that shaft needs to reduce.

Besides above, manufacturability of materials for ABS and PLA are changeable for process time and cost. PLA has better manufacturability and low cost requirement than PLA.

Comparison of all criteria as inner shaft, gear and main shaft with material configuration shows that optimum material for chassis must be PLA for low cost, manufacturability, suitability for both inner shaft and gear. In addition, for next revisions, main gear materials could be selected a material that has lower strength or with smaller diameter.

In the light of these information, conclusions of this study are:

- For designed ladder climbing robot, optimum chassis material is determined as PLA.
- Inner and outer shafts and couplings should be manufactured by S 235 steel.

- Transmission system for ladder climbing robot should be manufactured from PLA.
- Power consumption of ladder climbing robot that is manufactured from PLA will be about 67.5 Watt with consideration of safety.



6. RECOMMENDATIONS AND FUTURE WORKS

By further developments and improvements the listed below are recommended:

1. Main shaft diameter or material of the system can be optimized for next generation designs according to PLA based robot structural.
2. Designed system can be improved with adaptive leg length for different size of ladder dimensions.
3. Alternative transmission systems for ladder climbing robot can be comprised and optimized.

As future research directions:

1. It is planned to create adaptive leg length that can change instantaneously for different obstacle or ladder dimensions.
2. Bevel gear based or chain or belt based transmission system can be designed to obtain ladder climbing transmission system with less energy lose and more efficiency.

Developed robot structure can be used with LIDAR and robotic mapping capability to work in domestic or industrial environments for safety purposes

REFERENCES

- Arkin, R.C. (Ed.) 1998. Whence Behaviour? In: Behaviour Based on Robotics, Massachusetts Institute of Technology pp.1-28, United States of America.
- Ashby, M. F. 2011. Materials Selection in Mechanical Design (Fourth Ed.), Oxford: Elsevier Butterworth-Heinemann.
- Behnke, S. 2008. Humanoid Robots From Fiction to Reality. **CiteSeer**, pp.5-9.
- Boston Dynamics, [Online]. Available: <https://www.bostondynamics.com/sandflea>. [Accessed 11 September 2019].
- Breazeal, C., Berlin, M., Brooks, A., Gray, J., Thomaz, A.L. 2006. Using perspective taking to learn from ambiguous demonstrations. **Robotics and Autonomous Systems**, 54: 385-393.
- Brooks, R.A., Flynn, A.M. 1989. Fast, cheap and out of control: A robot invasion of the solar system. **Journal of the British Interplanetary Society**, 42: 478-485.
- Cabrita, G., Madhavan, R., Marques, L. 2015. A Framework for Remote Field Robotics Competitions. Autonomous Robot Systems and Competitions (ICARSC), 2015 IEE International Conference on. IEEE.
- Ceccarelli, M., Carbone, G. 2005. Legged Robotic Systems. In: Cutting Edge Robotics (Vedran, K., Aleksandar, L., Munir, M.), InTech, pp. 553-576, Germany.
- Chen, X.Q., Chen, Y.Q., Chase, J.G. (Eds.) 2009. Mobiles Robots – Past Present and Future. In: Mobile Robots - State of the Art in Land, Sea, Air, and Collaborative Missions, InTech, pp.1-32.
- Cook, G. 2011. Mobile Robots: Navigation, Control and Remote Sensing. Wiley, New Jersey.
- Durán, B., Thill, S. 2012. Rob's Robot: Current and Future Challenges for Humanoid Robots. In: The Future of Humanoid Robots - Research and Applications (Riadh, Z.), InTech, pp. 280-300.
- Garcia, E., Jimenez, M., De Santos, P., Armada, M. 2007. The Evolution of Robotics Research. **Robotics & Automation Magazine, IEEE**, 14: 90-103.
- Geppert, L. 2014. The Robot That Could. **Spectrum, IEEE**, 41:34-37.

- Hahnel, D., Triebel, R., Burgard, W., Thrun, S. 2003. Map Building with Mobile Robots in Dynamic Environments. International Conference on Robotics and Automation, IEEE, pp. 1557 - 1563.
- Hirose, S., Kato, K. 2000. Study on Quadruped Walking Robot in Tokyo Institute of Technology-Past, Present and Future. International Conference on Robotics and Automation, IEEE, pp.414-149, San Francisco.
- Hobbelen, D.G.E., Wisse, M. 2007. Limit Cycle Walking. In: Humanoid Robots, Human-like Machines (Matthias, H.), InTech, pp.278-294, China.
- IFR World Robotics, [Online]. Available: <https://ifr.org/downloads/press2018/Executive%20Summary%20WR%202019%20Industrial%20Robots.pdf>. [Accessed 11 September 2019].
- ISO 8373:2012, Robots and robotic devices. Available: <https://www.iso.org/obp/ui/#iso:std:iso:8373:ed-2:v1:en>. [Accessed 20 August 2019].
- Kar, D.C. 2003. Design of Statically Stable Walking Robot: A Review. **Journal of Robotic Systems**, 11:671-686.
- Karl, M.(Ed.) 2010. Industrial Robotics. In Robotics for Electronic Manufacturing, Cambridge University Press, pp.1-11, New York.
- Lim, H-O., Takanishi, A. (Eds.) 2006. Mechanism and Control of Anthropomorphic Biped Robots. In: Mobile robots, moving intelligence, InTech, pp. 308-324, Austria.
- Lund, H.H., Miglino O. 1996. From Simulated to Real Robots. International Conference on Evolutionary Computation, IEEE, pp. 362 - 365, Nagoya.
- Marques, L., Almeida, A. T., Armada, M., Fernández, R., Montes, H., González P., Baudoin, Y. 2012. State of the Art Review on Mobile Robots and Manipulators for Humanitarian Demining. In IARP WS on Humanitarian Demining, Sibenik, Croatia.
- Mars rover, [Online]. Available: <https://mars.nasa.gov/mer/>. [Accessed 11 September 2019].
- Matsui, D., Minato, T., MacDorman, K.F., Ishiguro, H. 2005. Generating Natural Motion in an Android by Mapping Human Motion. International Conference on Intelligent Robots and Systems, IEEE, pp. 3301-3308.

- Minato, T., Yoshikawa, Y., Noda, T., Ikemoto, S., Ishiguro, H., Asada, M. 2007. CB2 A Child Robot with Biomimetic Body for Cognitive Developmental Robotics. International Conference on Humanoid Robots, IEEE, pp. 557-562, Pittsburgh.
- Narukawa, T., Yokoyama, K., Takahashi, M., Yoshida, K. 2010. An experimental study of three dimensional passive dynamic walking with flat feet and ankle springs. In: Cutting Edge Robotics (Vedran, K.), InTech, pp.132-144, China.
- NASA, [Online]. Available: <https://www.botmag.com/pioneer-helps-chernobyl-clean/>. [Accessed 11 September 2019].
- Nehmzow, U. (Ed.) 2003. A Practical Introduction. In: Mobile Robotics, Springer pp. 25-45, New York.
- Nishio, S., Ishiguro, H., Hagita, N. 2007. Geminoid: Teleoperated Android of an Existing Person. In: Humanoid Robots: New Developments (Armando C.P. F.), InTech, pp.344-352, China.
- Nonami, K., Barai, R.K., Irawan, A., Daud, M.R. (Eds.) 2014. Historical and Modern Perspective of Walking Robots. In: Hydraulically Actuated Hexapod Robots, Springer, pp.19-40, New York.
- Ozguner, F., Tsai, S.J. 1985. Design and Implementation of a Binocular-Vision System for Locating Footholds of a Multi-Legged Walking Robot. **Neural Networks, IEEE Transactions**, 32:26-31.
- Park, W., Kim, J.Y., Lee, J., Oh, J.H. 2005. Mechanical Design of Humanoid Robot Platform KHR-3 (KAIST Humanoid Robot-3:HUBO). International Conference on Humanoid Robots, IEEE, pp.321-326, Tsukuba.
- Pavlak, A. 2016. Material Selection Analysis for the Development of an Integrated Surface Vehicle System. A thesis submitted to the University Honors Program in partial fulfillment of the requirements for the Honors Diploma, Southern Illinois University, Illinois, USA.
- Reeve, R., Hallam J. 2005. Analysis of Neural Models for Walking Control. **Neural Networks, IEEE Transactions**, 16:733-742.
- Richardson, K. 2008. The fact and fiction of robots. **The Thinking Machine**, University of Cambridge.
- Robotic Universe, Materials for Robot Building: An Introduction. 2019. [Online]. Available: <http://www.robotoid.com/howto/materials-for-robot-building-an-introduction.html>. [Accessed 11 September 2019].

- Rosheim, M.E. (Ed.) 1994. Robots past. In: Robot Evolution: The Development of Anthrobotics, Wiley & Sons, Inc., pp.1-37, New York, USA.
- Saga Robotics, [Online]. Available: <https://sagarobotics.com/blogs/news/162130055-w-series-br-working-horse-purepower>. [Accessed 11 September 2019].
- Sciavicco, L., Siciliano, B. (Eds.) 2005. Robotics. In: Modelling and Control of Manipulators, McGraw Hill, pp.1-16, London.
- Shadow Robot Company [Online]. Available: <http://www.shadowrobot.com/products/dexterous-hand/>. [Accessed 11 September 2019].
- Silva, M.F., Machado, J.A.T. 2007. A Historical Perspective of Legged Robots. **Journal of Vibration and Control**, 20: 1378-1393.
- Thrun, S., Montemerlo, M., Dahlkamp, H., Stavens, D., Aron, A., Diebel, J., Fong, P., Gale, J., Halpenny, M., Hoffmann, G., Lau, K., Oakley, C., Palatucci, M., Pratt, V., Stang, P. 2006. Stanley: The Robot that Won the DARPA Grand Challenge. **Journal of Field Robotics**, pp. 661-692.
- Valgren, C. 2007. Incremental Spectral Clustering and Its Application To Topological Mapping. International Conference on Robotics and Automation, IEEE, pp. 4283-4288, Roma.
- Vukobratovic, M., BOROVIAC B. 2004. Zero Moment Point Thirty five years of its life. **International Journal of Humanoid Robotics**, 1:157-173.
- Wallén, J. 2008. Estimation-based iterative learning control. Department of Electrical Engineering Linköping University, Ph.D. Thesis, Linköping.
- Wallgörn, J. O. 2010. Hierarchical Voronoi Graphs: Spatial Representation and Reasoning for Mobile Robots. Springer.
- Zielinska, T. 2004. Development of a walking machine: mechanical design and control problems. **Mechatronics**, 12:737-754.

APPENDICES

Appendix 1 (Matlab Scripts)

Motion Calculations

```

%Acceleration and Force Calculations%

%Check for rolling

%F=m*a;

%m*a=m*g*sin(thetal*pi/180)-Ffr;

%T=I*alpha

%alpha=a/r;

%Ffr*r=1/2*m*r^2*(a/r);

%Ffr=1/2*m*a;

%m*a=m*g*sin(thetal*pi/180)-1/2*m*a;

%a=2*Ffr/m;

%a=2*g*cos(thetal*pi/180)*M;

%Fmax-Ffr=m*a;

%Fmax-1/2*(m*a)=m*a;

%Fmax=3/2*(m*a);

%Fs=m*g*sin(thetal*pi/180);

%If Fmax>Fs; rolling is ok there is no slippage;

m=10.5; % kg, weight of total system

cfr=0.75; % cfr, coefficient of static friction

```

```

g=9.81; % m/s^2, standard earth gravity

thetar=30; % degree, slope angle of ladder

r= 0.21; % m, radius of total system

amax=2*g*cosd(thetar)*cfr; % m/s^2, translational acceleration

Ffr=1/2*(m*amax); % N, friction force

Fs=m*g*sind(thetar); % N, slippage force

Fmax=3/2*(m*amax); % N,

%Rolling Motion

%Acceleration and Torque

%T=I*alpha

%alpha=ar/r;

%Ffr*r=1/2*m*r^2*(ar/r);

%Ffr=1/2*m*ar;

m*g*cos(thetal*pi/180)*M=1/2*m*ar

%M=ar/2*g*cos(thetal*pi/180);

%F=m*ar;

m*ar=m*g*sin(thetal*pi/180)-m*g*cos(thetal*pi/180)*M;

%ar=2/3*g*sin(thetal*pi/180);

ar=2/3*g*sind(thetar);

%Torque Calculations for rolling motion

%Total Moment I*alpha+m*ar*r

```

76

%Meq=Total moment=T

%alpha=ar/r

%I=m*r^2

%I for cylinder 1/2*m*r^2

%M=(1/2*m*r^2)*(a/r)+(m*ar*r)

%T=M=3/2*(m*r*ar)

alpha=ar/r; % rad/s^2, angular acceleration

I=1/2*m*r^2; % kg*m^2, moment of inertia

Tr=3/2*(m*r*ar); % Nm, Total torque

Thr=Tr/2; % torque for one half

% Angular speed, power(rolling)

v=1; % m/s, linear velocity of the system

ws=v/r; % rad/s, angular velocity of system

rpms=(ws*60)/(2*pi); % rpm,

Pr=Tr*ws; % Watt, required power for system

Phr=Pr/2; % Watt, power for one half

%Linear motion forces

rw=0.06; % m, radius of wheel;

al=0; % m/s^2, translational acceleration;

crol=0.02; % rolling coefficient;

thetap=20 ; % degree, slope angle of path;


```

Ftr=m*g*cosd(thetap); % traction force;

Fg=m*g*sind(thetap); % N, gradient resistance;

Frol=m*g*crol; % N, rolling resistance;

Fa=m*al; % N, acceleration resistance;

Fdrv=Fg+Frol+Fa; % N, sum of the forces;

% Angular speed, power (linear)

v=1; % m/s, linear velocity of the system

w=v/rw; % rad/s, angular velocity of outer gear

ro=0.03; % m, radius of outer gear

rm=0.06; % m, radius of main gear

e= 0.8; %

wo=w; % rad/s, angular velocity of outer gear

wm=wo*ro/rm; % rad/s, angular velocity of main gear

rpm=(wm*60)/(2*pi); % rpm,

Tl=m*g*(sind(thetap)+(cfr))*rw; %Nm total torque

Thl=Tl/2; %Nm torque for one half

Pl=Fdrv*v/e; % Watt, required power for system

Phl=Pl/2; % Watt, power for one half

%Power supply

Ab=3; % Ah, ampere hour

Vb=14.8; % V, voltage

```

78

Pb=Ab*Vb; % Wh, Energy

fprintf('Rolling motion\n');

fprintf('Check for rolling\n');

fprintf('amax = %4.2f m/s^2\n',amax);

fprintf('Forces\n');

fprintf('Ffr = %4.2f N\n',Ffr);

fprintf('Fs = %4.2f N\n',Fs);

fprintf('Fmax = %4.2f N\n',Fmax);

if Fmax > Fs

fprintf('No slippage\n');

else

fprintf('slippage\n');

end

fprintf('ar = %4.2f m/s^2\n',ar);

fprintf('Rolling torque\n');

fprintf('I = %4.2f kgm^2\n',I);

fprintf('Tr = %4.2f Nm\n',Tr);

fprintf('Thr = %4.2f Nm\n',Thr);

fprintf('Angular speed and power\n');

fprintf('ws = %4.2f rad/s\n',ws);

fprintf('rpms = %4.2frpm\n',rpms);

```
fprintf('Pr = %4.2f W\n',Pr);  
  
fprintf('Phr = %4.2f W\n',Phr);  
  
fprintf('Linear motion\n');  
  
fprintf('Forces\n');  
  
fprintf('Ftr = %4.2f N\n',Ftr);  
  
fprintf('Fg = %4.2f N\n',Fg);  
  
fprintf('Frol = %4.2f N\n',Frol);  
  
fprintf('Fa = %4.2f N\n',Fa);  
  
fprintf('Fdrv = %4.2f N\n',Fdrv);  
  
if Ftr > Fdrv  
  
    fprintf('No slippage\n');  
  
else  
  
    fprintf('slippage\n');  
  
end  
  
fprintf('Angular speed and power\n');  
  
fprintf('w = %4.2f rad/s\n',w);  
  
fprintf('wo = %4.2f rad/s\n',wo);  
  
fprintf('wm = %4.2f rad/s\n',wm);  
  
fprintf('rpm = %4.2frpm\n',rpm);  
  
fprintf('Tl = %4.2f Nm\n',Tl);  
  
fprintf('Thl = %4.2f Nm\n',Thl);
```

80

```
fprintf('Pl = %4.2f W\n',Pl);
```

```
fprintf('Phl = %4.2f W\n',Phl);
```

```
fprintf('Power supply\n');
```

```
fprintf('Pb = %4.2f Wh\n',Pb);
```

Mechanical Strength Check of the Components

```
clc
```

```
%Main shaft minimum diameter%
```

```
%the affected forces on the gear Ftm, Fnm, Frm
```

```
%alpha is the clutch angle 20 degree
```

```
%dm is diameter of main gear
```

```
%Mr is rotation moment
```

```
Mr=6; %Nm
```

```
alpha=20; %degree
```

```
dm=0.120; %m
```

```
Ftm=(2*Mr/dm);
```

```
Fnm=Ftm/cosd(alpha);
```

```
Frm=Ftm*tand(alpha);
```

```
%Forces act on the xy plane and bearings
```

```
%AB,AC and BC are the distances on the shaft
```

```
% sum moment at A=0
```

```
% Fnm*dm/2+Frm*AC-Fby*AB=0
```

AB=50; %mm

AC=35; %mm

BC=15; %mm

FBy=(Fnm*dm*1000/2+Frm*AC)/AB; %N

%FAy+FBy=Frm

if Frm > FBy

FAy=(Frm-FBy);

else

FAy=(Frm-FBy)*-1; %because of the direction of the forces

end

%Bending Moment at C point for xy

MBc1=(FAy*AC)/1000;

if (FAy*AC/1000)>(Fnm*dm/2)

MBc2=[(FAy*AC/1000)-(Fnm*dm/2)];

else

MBc2=[(FAy*AC/1000)-(Fnm*dm/2)]*-1;

end

%Forces act on the xz plane and bearings

% sum moment at A=0

%Ftm*AC-FBz*50=0

FBz=Ftm*AC/50;

82

FAz=Ftm-FBz;

%Bending Moment at C point for xz

MBc3=(FAz*AC)/1000;

%Resultant forces at A and B bearings

FAr=(FAy^2+FAz^2)^(1/2);

FBr=(FBy^2+FBz^2)^(1/2);

%Resultant bending moment

MBr=(MBc1^2+MBc3^2)^(1/2); %Nm

%Shaft diameter

qTDE=180; %N/mm^2 for S235 steel, Fully variable strength of material

Re= 235; %N/mm^2 yield strength

Kb=0.95; % shape coefficient

Ky=0.9; % surface coefficient

Kc=1.2; % notch effect

S=3; % safety factor

t1=6; %depth of key or pin

qTDE=qTDE*Kb*Ky/Kc; %under dynamic loads

d=[32*S/pi*((MBr*1000/qTDE)^2+(3/4*Mr*1000/Re)^2)^(1/2)]^(1/3);

d=d+t1;

fprintf('Main Shaft\n');

fprintf('Ftm = %4.2f N\n',Ftm);

```

fprintf('Fnm = %4.2f N\n',Fnm);

fprintf('Frm = %4.2f N\n',Frm);

fprintf('FBy = %4.2f N\n',FBy);

fprintf('FAy = %4.2f N\n',FAy);

fprintf('MBc1 = %4.2f Nm\n',MBc1);

fprintf('MBc2 = %4.2f Nm\n',MBc2);

fprintf('FBz = %4.2f N\n',FBz);

fprintf('FAz = %4.2f N\n',FAz);

fprintf('MBc3 = %4.2f Nm\n',MBc3);

fprintf('FAr = %4.2f N\n',FAr);

fprintf('FBr = %4.2f N\n',FBr);

fprintf('MBr = %4.2f Nm\n',MBr);

fprintf('d = %3.2f mm\n',d);

%outer shaft minium diameter%

do=0.060; %m

Mr=Mr*(do/dm); %Nm

Fto=(2*Mr/do);

Fno=Fto/cosd(alpha);

Fro=Fto*tand(alpha);

%Forces act on the xy plane and bearings

%AB,AC and BC are the distances on the shaft

```

84

% sum moment at A=0

% $F_{ni} \cdot d_i/2 + F_{ri} \cdot AC - F_{by} \cdot AB = 0$

AB=50; % mm

AC=35; % mm

BC=15; % mm

FBy=(Fno*do*1000/2+Fro*AC)/AB; % N

% F_{Ay}+F_{By}=F_{rm}

if Fro > FBy

F_{Ay}=(Fro-FBy);

else

F_{Ay}=(Fro-FBy)*-1; % because of the direction of the forces

end

% Bending Moment at C point for xy

MBc1=(F_{Ay}*AC)/1000; % Nm

if (F_{Ay}*AC/1000)>(Fno*do/2)

MBc2=[(F_{Ay}*AC/1000)-(Fno*do/2)];

else

MBc2=[(F_{Ay}*AC/1000)-(Fno*do/2)]*-1;

end

% Forces act on the xz plane and bearings

% sum moment at A=0

$$\%F_{tm} \cdot AC - F_{Bz} \cdot 50 = 0$$

% Bending Moment at C point for xy

$$F_{Bz} = F_{to} \cdot AC / 50;$$

$$F_{Az} = F_{to} - F_{Bz};$$

% Bending Moment at C point for xz

$$M_{Bc3} = (F_{Az} \cdot AC) / 1000;$$

% Resultant forces at A and B bearings

$$F_{Ar} = (F_{Ay}^2 + F_{Az}^2)^{(1/2)};$$

$$F_{Br} = (F_{By}^2 + F_{Bz}^2)^{(1/2)};$$

% Resultant bending moment

$$M_{Br} = (M_{Bc1}^2 + M_{Bc3}^2)^{(1/2)}; \% Nm$$

$$d = [32 \cdot S / \pi \cdot ((M_{Br} \cdot 1000 / q_{TDE})^2 + (3/4 \cdot M_r \cdot 1000 / R_e)^2)^{(1/2)}]^{(1/3)};$$

$$t_2 = 2;$$

$$d = d + t_2;$$

fprintf('Outer Shaft\n');

fprintf('Fto = %4.2f N\n', Fto);

fprintf('Fno = %4.2f N\n', Fno);

fprintf('Fro = %4.2f N\n', Fro);

fprintf('FBy = %4.2f N\n', FBy);

fprintf('FAy = %4.2f N\n', FAy);

fprintf('Mbc1 = %4.2f Nm\n', Mbc1);

86

```
fprintf('MBc2 = %4.2f Nm\n',MBc2);
```

```
fprintf('FBz = %4.2f N\n',FBz);
```

```
fprintf('FAz = %4.2f N\n',FAz);
```

```
fprintf('MBc3 = %4.2f Nm\n',MBc3);
```

```
fprintf('FAr = %4.2f N\n',FAr);
```

```
fprintf('FBr = %4.2f N\n',FBr);
```

```
fprintf('MBr = %4.2f Nm\n',MBr);
```

```
fprintf('d = %3.2f mm\n',d);
```

```
clc
```

```
%Gear main dimensions
```

```
%p=pitch
```

```
%d=pitch diameter
```

```
%da=major diameter
```

```
%s=pitch thickness
```

```
%b=pitch width
```

```
%m=module =p/pi
```

```
%z= number of teeth
```

```
%alpha=clutch angle generally 20 degree
```

```
%minimum number of teeth is theoretically 17
```

```
%Basic equations
```

$\%d=m*z$

$\%p=m*pi$

$\%$ Check according to broken at pitch bottom

$R_m=35$; $\%$ UTS MPa

$R_e=30$; $\%$ Yield MPa

$K_b=1$; $\%$ shape coefficient

$K_y=0.75$; $\%$ surface coefficient

$K_c=1.2$; $\%$ notch effect

$S=3$; $\%$ safety factor

$\%$ As the PLA brittle plastic material, continuous strength of the material was assumed equal to R_e .

$\%q_{TD}$ = pure variable strength

$q_{Fe}=R_e$;

$q_{TD}=R_e*0.7$;

$q_s=(K_b*K_y*q_{TD})/(K_c*S)$;

$\%$ Module Check (m)

$M_r=3$; $\%$ Nm

$K_f=2.4$; $\%$ form coefficient

$K_i=1.25$; $\%$ operation coefficient

$K_v=1$; $\%$ speed coefficient

$K_e=1$; $\%$ clutch ratio coefficient

88

$K_m=1.2$; %Load dist. coefficient

$S=3$; %safety factor

$w_m=15$; %module width coefficient it can selected between 10-20

$z=20$; %number of teeth

$\beta=20$; %beta

$m_n = [(2 * M_r * 1000 * K_f * K_i * K_v * K_e * K_m) / (w_m * z * q_s * \cos(\beta))]^{1/3}$;

$m_a = [m_n / \cos(\beta)]$;

fprintf('Gear check\n');

fprintf('Check according to broken at pitch bottom \n');

fprintf('q_s= %4.2f N/mm²\n',q_s);

fprintf('m_n= %4.2f mm\n',m_n);

fprintf('m_a= %4.2f mm\n',m_a);

% as the calculated value was found as 2.49 module was determined as 3.

%Check according to surface pressure

%q_H= continous surface pressure strength

%K_p= pressure coefficient

q_H=Re;

K_p=1;

P_s=q_H*K_p/S;

% Module Check

E=1100; %Elastic modulus of material MPa

```

i12=2; %rotation ratio

mn=[2*Mr*1000*Ki*Kv*Km*Ke*E*(i12+1)/(wm*z^2*Ps^2*i12)]^(1/3)*(cosd(b
eta));

ma=[mn/cosd(beta)];

fprintf('Check according to surface pressure \n');

fprintf('Ps= %4.2f N/mm^2\n',Ps);

fprintf('mn= %4.2f mm\n',mn);

fprintf('ma= %4.2f mm\n',ma);

% as the calculated value was found as 2.74 module was determined as ok.

% Pitch thickness check

m=3;

p=pi*m;

d=m*z;

dr=d+2*m;

s=p/2;

alpha=20; %degree

cosr= d*cosd(alpha)/dr; %clutch angle at related angle

alphan=acosd(cosr);

invr = tand(alphan)-alphan*pi/180;

inv20=0.01490; %inv value for 20 degree

sr=dr*[s/d+(0.01490-invr)] ;

```

90

```
srmin= 0.4*m;
```

```
fprintf('tooth thickness check \n');
```

```
fprintf('sr= %4.2f mm\n',sr);
```

```
fprintf('srmin= %4.2f mm\n',srmin);
```

```
% as the calculated sr is more than srmin gear set is ok.
```

```
clc
```

```
% Stud Diameter Check
```

```
Mr=6; %Nm
```

```
D0=17; % Inner diameter
```

```
z=2; %Number of stud
```

```
Ft=(2*Mr*1000)/(z*D0); % Tangential force
```

```
b=6; % Wall thickness of coupling
```

```
Rs=350; % Yield strength of stud material
```

```
S=3;
```

```
Mb=(16*Ft*b); % Bending moment
```

```
% Wb=(pi*dp^3) Bending moment strength mm^3
```

```
% qs=Mb*S/Wb*Rs Safe stress value
```

```
dp=[(S*Mb)/(pi*Rs)]^(1/3);
```

```
Wb=(pi*dp^3);
```

```
qs=Mb/Wb;
```

```
% as the minimum diameter was calculated 4.5 diameter was selected as 5.
```

```
fprintf('Stud Diameter Check\n');
```

```
fprintf('Ft = %4.2f N\n',Ft);
```

```
fprintf('Mb = %4.2f Nm\n',Mb);
```

```
fprintf('Wb = %4.2f mm^3\n',Wb);
```

```
fprintf('qs = %4.2f N/mm^2\n',qs);
```

```
fprintf('dp = %4.2f mm\n',dp);
```

RESUME

Personel Information

Name Surname : Ogulcan TURHANLAR

Place and Date of Birth : 10.05.1994

Education

Undergraduate : B.Sc. degree at Aydın Adnan Menderes University

Foreign Languages : English

Scientific Activities

A) Papers in Referred Journals

1. Bogrekci, I., Sucuoglu, H. S., Demircioglu, P., Turhanlar, O. (2018). Structural Analysis of Corn Silo by Computing Vertical and Lateral Forces. **Acta Technica Napocensis Series-Applied Mathematics Mechanics and Engineering**, 61(4), 423-428. (Yayın No: 5493763).
2. Bogrekci, I., Sucuoglu, H. S., Demircioglu, P., Turhanlar, O., Gültekin A. (2018). Structural and Discrete Element Analysis of Coal Mine Conveyor System. **Acta Technica Napocensis Series-Applied Mathematics Mechanics and Engineering**, 61(4), 429-434. (Yayın No: 5493846).
3. Sucuoglu, H. S., Bogrekci, I., Gültekin A., Demircioglu, P., Turhanlar, O. (2018). Development of Hybrid Pattern for Three Dimensional Printing Optimization. **Sigma**, 36(3) (Yayın No: 4507713).
4. Sucuoglu, H. S., Bogrekci, I., Demircioglu, P., Turhanlar, O. (2016). Analysis of Suspension System for 3d Printed Mobile Robot. **International Journal of Applied Mathematics, Electronics and Computers** (Yayın No: 3277593).

B) Proceedings

1. Sucuoglu, H. S., Bogrekci, I., Demircioglu, P., Turhanlar, O. (2017). Design, Analysis and Manufacturing of Multipurpose Cylindrical Shape Robot. 6th International Conference on Advanced Technology Sciences (Tam Metin Bildiri/Sözlü Sunum)(Yayın No:3586136).

2. Sucuoglu, H. S., Bogrekci, I., Demircioglu, P., Turhanlar, O. (2016). Analysis of Suspension System for 3d Printed Mobile Robot. International Conference on Advanced Technology Sciences, ICAT'16. In: Proceedings of the 3th International Conference on Advanced Technology Sciences (Tam Metin Bildiri/Sözlü Sunum)(Yayın No:3179844).

C) Book Chapters

1. Advanced Mechatronics Solutions, Bölüm adı:(Design & FEA and Multi Body System Analysis of Human Rescue Robot Arm) (2016)., SUCUOĞLU HİLMİ SAYGIN, BÖĞREKÇİ İSMAİL, DEMİRCİOĞLU PINAR, TURHANLAR OĞULCAN, Springer International Publishing, Editör:Ryszard Jabłoński, Tomas Brezina, Basım sayısı:1, Sayfa Sayısı 6, ISBN:978-3-319-23921-7, İngilizce(Bilimsel Kitap), (Yayın No: 1717841).

C) Projects

1. Güvenlik ve Arama Kurtarma Amaçlı Çoklu Mobil Robot Sisteminin Geliştirilmesi, Yükseköğretim Kurumları tarafından destekli bilimsel araştırma projesi, Yürütücü: DEMİRCİOĞLU PINAR, Araştırmacı: BÖĞREKÇİ İSMAİL, Araştırmacı: SUCUOĞLU HİLMİ SAYGIN, Araştırmacı: GÜLTEKİN AŞLI, Araştırmacı:TURHANLAR Oğulcan, Araştırmacı:EMANET Cihat Göktuğ, , 10/03/2017 (Devam Ediyor) (ULUSAL).
2. Binalarda Enerji Verimliliği Amaçlı Kullanılacak İnsansız Hava Aracı (İHA) Sisteminin Geliştirilmesi, Yükseköğretim Kurumları tarafından destekli bilimsel araştırma projesi, Yürütücü: BÖĞREKÇİ İSMAİL, Araştırmacı:DEMİRCİOĞLU PINAR, Araştırmacı:AKKOYUN FATİH, Araştırmacı: SUCUOĞLU HİLMİ SAYGIN, Araştırmacı:GÜLTEKİN AŞLI,Araştırmacı:TURHANLAR Oğulcan, 10/03/2017 (Devam Ediyor) (ULUSAL).

Contact

E-mail : ogulcan.turhanlar@gmail.com

Date :13/01/2020